

Stony Brook University



OFFICIAL COPY

The official electronic file of this thesis or dissertation is maintained by the University Libraries on behalf of The Graduate School at Stony Brook University.

© All Rights Reserved by Author.

**Analysis of the Interaction of H-NOX with DGC using *in vivo* methods and Analytical
Ultracentrifugation**

A Thesis Presented

by

Patryk Zielinski

to

The Graduate School

in Partial Fulfillment of the

Requirements

for the Degree of

Master of Science

in

Chemistry

Stony Brook University

August 2013

Copyright by
Patryk Zielinski
2013

Stony Brook University

The Graduate School

Patryk Zielinski

We, the thesis committee for the above candidate for the
Master of Science degree, hereby recommend
acceptance of this thesis.

Elizabeth M. Boon, Ph.D., Thesis Advisor

Assistant Professor, Department of Chemistry

Stephen A. Koch, Ph.D., Committee Chair

Professor, Department of Chemistry

Dale G. Drueckhammer, Ph.D., Third Member

Professor, Department of Chemistry

This thesis is accepted by the Graduate School

Charles Taber
Interim Dean of the Graduate School

Abstract of the Thesis

Analysis of the Interaction of H-NOX with DGC using *in vivo* methods and Analytical

Ultracentrifugation

by

Patryk Zielinski

Master of Science

in

Chemistry

Stony Brook University

2013

Biofilms are a naturally occurring phenomenon and are known to be a significant problem in various fields including both the industrial and health environments. Bacterial biofilms are defined as the attachment and aggregation of a community of bacteria to solid surfaces. This behavior can lead to infections via medical transplants and compromise the functionality and durability of industrial equipment. Two proteins, *Heme-Nitric oxide/Oxygen* (H-NOX) and di-guanylate cyclase (DGC), are known to play an important role in the regulation of biofilm formation in bacteria. These two proteins down regulate the concentration of c-di-GMP, a second messenger molecule, in a cell. Since c-di-GMP has been shown to directly affect a cell's motile state, further studies on the H-NOX and DGC proteins may bring about an understanding of possible ways to artificially manipulate their biological roles.

Shewanella woodyi (*S.woodyi*) is a marine bacterium which contains the genes encoding for H-NOX and DGC and, additionally, has been observed to participate in biofilm formation.

Recent *in vitro* studies have shown that H-NOX directly interacts with DGC to regulate its cyclase and phosphodiesterase activities. In one study we aim to show this direct interaction using *in vivo* methods involving the re-introduction of tagged equivalents of these two genes, via a broad host range vector, into a mutant strain of *S.woodyi* lacking these two proteins. The experimental design is centered on using the native ribosome binding site of the genes encoding for H-NOX and DGC for the *in vivo* expression of these two proteins in the mutant *S.woodyi* organism. Multiple tests for the detection of these two proteins from the *S.woodyi* complements were performed with an observed absence of the presence of either of the two proteins. These results indicate that either the lack of efficiency of plasmid replication and/or the occurrence of random mutations is possible.

Since DGC is a complex protein containing three domains, two of which are enzymatically active, we decided to perform another study involving the isolation and purification of each of these domains to examine their behavior in the absence of the other two proteins. We also wanted to observe which domains were capable of interacting with the H-NOX protein. Currently we have successfully analyzed the oligomeric state of the EAL, EAL with H-NOX, and PAS proteins and assessed the lack of activity for the isolated EAL and GGDEF proteins. Future tests will be performed to study the oligomeric state of the GGDEF protein (in the presence and in the absence of H-NOX) and PAS in the presence of H-NOX.

Table of Contents

List of figures/tables.....	vii
List of abbreviations.....	ix
1: Background.....	1
1.1 Nitric Oxide.....	1
1.2 H-NOX.....	2
1.3 DGC.....	3
1.4 Biofilms.....	4
1.5 <i>Shewanella woodyi</i>	5
2: Progress towards Analysis of H-NOX interaction with DGC using <i>in vivo</i> methodology.....	6
2.1 Abstract.....	6
2.2 Introduction.....	6
2.3 Methods.....	8
2.4 Results and Discussion.....	16
3: Analysis of the Interaction of isolated DGC motifs with HNOX using Analytical Ultracentrifugation.....	30
3.1 Abstract.....	30
3.2 Introduction.....	30
3.3 Methods.....	31
3.4 Results and Discussion.....	33
References.....	44
Appendix.....	46

List of Figures/Tables

Figure 1-1 DGC cyclase and phosphodiesterase domain functions

Figure 1-2 Correlation between cellular c-di-GMP levels and biofilm formation

Figure 2-1 Agarose gel confirmation of *S.woodyi* DKO strain

Figure 2-2 Experimental constructs for *in vivo* study of H-NOX interaction with DGC

Figure 2-3 Developed Western Film for the expression of H-NOX-His from *E.coli* WM3064 strain

Figure 2-4 Developed Western Film for the expression of H-NOX-His from *S.woodyi* DKO *hnox*-His complement

Figure 2-5 Developed Western Film for the detection of purified H-NOX His at differing concentrations

Figure 2-6 Developed Western Film for the expression of H-NOX His from *S.woodyi* DKO *hnox*-His complement

Figure 2-7 Growth curve for *S.woodyi* DKO with and with NO

Figure 2-8 Growth curve for *S.woodyi* DKO pBBR1MCS-2 *hnox* His with and without NO

Figure 2-9 Ponceau'd western blot for the samples collected from the growth curve experiment

Figure 2-10 Developed Western Film for the expression of H-NOX-flag from *S.woodyi* DKO *hnox*-flag complement

Figure 2-11 Agarose gel for amplification of cDNA for the *hnox* gene from *S.woodyi* complements

Figure 2-12 Bar graph for the CV/OD calculation for phenotypic assays for the *S.woodyi* DKO complements

Figure 3-1 Circular Dichroism data for EAL, PAS, and GGDEF proteins

Figure 3-2 Coomassie-stained gel and developed western film for EAL

Figure 3-3 FPLC UV trace for EAL

Figure 3-4 AUC graph for EAL only run

Figure 3-5 AUC graph for EAL run with H-NOX

Figure 3-6 Activity Assay for EAL

Figure 3-7 FPLC UV trace for PAS

Figure 3-8 Coomassie-stained gel and developed western film for PAS

Figure 3-9 AUC graph for PAS only run

Figure 3-10 Coomassie-stained gel and developed western film for GGDEF

Figure 3-11 FPLC UV trace for GGDEF

Figure 3-12 Activity Assay for GGDEF

Table 2-1 DNA template and primers used for cloning *in vivo* experimental constructs

List of Abbreviations

NO – Nitric Oxide

S.woodyi – *Shewanella woodyi*

E.coli – *Escherichia coli*

WT – Wild type

DKO – Double Knockout

DAP – 2,6 Diaminopimelic acid

gDNA – genomic DNA

sGC – soluble guanylate cyclase

DGC – Di-guanylate cyclase

H-NOX – Heme-Nitric oxide/Oxygen

DPTA – Dipropylenetriamine NONOate

DEA – Diethylamine NONOate

Kan – Kanamycin

Amp – Ampicillin

Cam – Chloramphenicol

c-di-GMP – cyclic-di-GMP

pGpG – 5'-phosphoguanlyl-(3'-5')-guanosine

FPLC – Fast Protein Liquid Chromatography

HPLC – High Pressure Liquid Chromatography

AUC – Analytical Ultracentrifugation

Chapter 1: Background

1.1 Nitric Oxide

Nitric Oxide (NO) is a small diatomic gas molecule that functions as a first messenger molecule in a wide-range of biological processes in both prokaryotic and eukaryotic organisms (1). In addition to its function as an agent in the degeneration of tumor cells, NO has been shown to play a prominent role in the regulation of cellular apoptosis (2) as well as biological processes involving smooth muscle relaxation such as vasodilatation (3). NO has also been observed to be an important agent in the down regulation of cellular motility (4).

1.2 H-NOX

Heme-Nitric oxide/Oxygen (H-NOX) is a recently coined term which refers to the family of hemoproteins that have evolved to sense and bind small ligands and gas molecules. H-NOX contains a protoporphyrin IX heme group and is a bacterial homolog of the mammalian soluble guanylate cyclase (sGC) protein (5). Soluble guanylate cyclase is a protein of extensive study and has been shown to be involved, amongst other biological processes, in the vasodilation process in mammals (4). Specifically, sGC is a strong target of NO which, upon binding, activates sGC and results in a significant increase in the production of cGMP which then, in the case of vasodilation, causes smooth muscle relaxation. Similarly, H-NOX has been shown to also have a high affinity for NO (6).

1.3 DGC

Organisms which house an H-NOX gene usually contain either a di-guanylate cyclase gene (DGC) or a histidine kinase gene in the same operon (7). The DGC protein is interesting in the fact that it contains two enzymatically active domains. The cyclase domain is able to take two molecules of GTP to make one molecule of c-di-GMP, while the phosphodiesterase domain is able to take one molecule of c-di-GMP and break it down to pGpG (5'-phosphoguanylyl-(3'-5')-guanosine) (Figure 1-1). The activities of these two domains antagonize each other, making this protein capable of regulating the cellular concentration of c-di-GMP within a cell (8). *In vitro* studies have shown that H-NOX directly interacts with DGC to regulate its net activity. This interaction is upregulated by NO; Unbound H-NOX will allow the cyclase activity of DGC to remain dominant, while NO-bound H-NOX will alter the structure of DGC allowing the phosphodiesterase activity to become dominant.

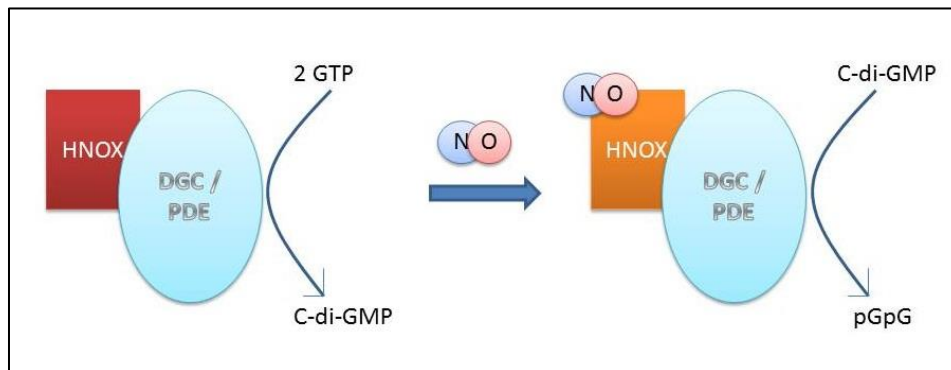


Figure 1-1. DGC can bind two molecules of GTP and convert them to c-di-GMP, a second messenger which is capable of triggering biofilm formation through a signaling cascade. However, if a first messenger (NO) binds H-NOX it will change its configuration (represented by the change in color from red to orange) and activate DGC's phosphodiesterase activity causing it to instead bind and breakdown c-di-GMP to pGpG, preventing biofilm generation.

1.4 Biofilms

Bacterial biofilms are defined as the attachment and aggregation of a community of bacteria to solid surfaces. It has been shown that increasing levels of c-di-GMP have a direct correlation with biofilm formation (9); high c-di-GMP levels correspond to a cell's sessile (immobile) state, while a low level of c-di-GMP promotes motility. Consequently high concentrations of c-di-GMP are known to promote the participation of bacteria in biofilms (Figure 1-2).

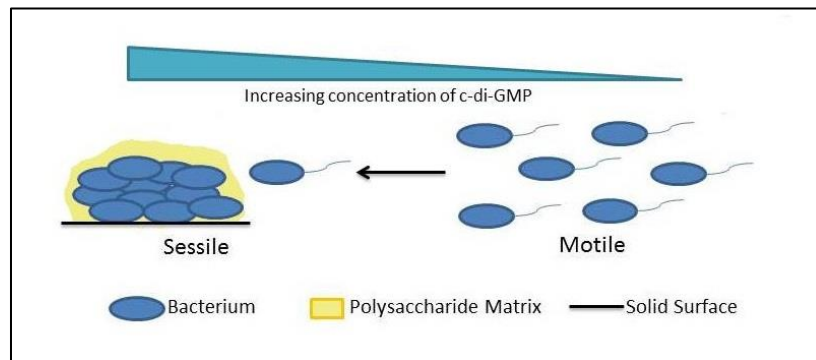


Figure 1-2. Cell motility decreases with increasing concentrations of c-di-GMP. Thus when H-NOX is unligated DGC produces and increases the cellular concentration of c-di-GMP causing the cells to enter a sessile state and attach to a solid surface, where the cells secrete a thick Polysaccharide Matrix which confers the biofilms their chemically impermeable nature.

Due to the thick polysaccharide matrix secreted by the sessile cells, biofilms show strong resistances to antibiotics, host immune responses, and various other chemical agents, making them both difficult to study directly and an expensive problem in both the industry and health environments (10). Whether it be biofilm formations occurring on medical implants, in the lungs of patients with cystic fibrosis, or on the hull of ships, biofilms are not only problematic in the damage they cause but also in the fact that they can grow in many different environments. Due to

this fact, biofilms have become an area of intensive research with hopes of understanding the mechanistic pathway of how biofilm formation is triggered and under what conditions.

1.5 *Shewanella woodyi*

Shewanella woodyi (*S.woodyi*) is an example of gram-negative luminescent marine bacteria which is capable of forming biofilm. Being a marine bacterium, the optimal growth temperature for this bacteria strain is in the range between 4⁰C and 25⁰C. Furthermore, *S.woodyi* is characterized by its rod-like morphology and its unsheathed polar flagellum (11). This particular bacterium contains the H-NOX and DGC proteins responsible for biofilm regulation. The H-NOX protein native to *S.woodyi* is molecularly biased for binding NO due to the protein's lack of specifically coordinated amino acids that usually help in stabilizing molecular oxygen (12).

Chapter 2: Progress towards Analysis of H-NOX interaction with DGC using *in vivo* methodology

2.1 Abstract

Biofilms are characterized by the attachment of a community of bacteria on biotic or abiotic solid surfaces. Nitric oxide (NO) is known to play a key role in bacterial biofilm formation (9). *Shewanella woodyi* is a biofilm-dwelling marine bacterium with an H-NOX domain that serves as the primary NO sensor. NO-bound H-NOX has been shown to regulate the enzymatic activity of an associated diguanylate cyclase/phosphodiesterase protein (DGC) (13), consequently regulating the production of cyclic di-GMP. Cyclic di-GMP is well known for triggering biofilm formation (14). H-NOX and DGC interaction has been established *in vitro*, here we attempt to evaluate the H-NOX and the DGC interaction *in vivo* using a knockout mutant that lacks both proteins (*S.woodyi* DKO). The aim was to re-introduce the two proteins using a broad-host range vector into the *S.woodyi* DKO strain and to have the bacteria use the native ribosome binding sites to transcribe and translate both proteins. The interaction of these two proteins could then be shown using a technique called immunoprecipitation. The methods and results of this approach will be presented.

2.2 Introduction

It has been shown using *in vitro* methods that H-NOX directly interacts with the DGC protein to regulate its function (15). The aim of this study was to design several constructs which would allow us to test this interaction under *in vivo* conditions using a technique known as protein complex immunoprecipitation (Co-IP). This technique depends on a known protein and the use of an antibody which targets the known protein. The antibody is then used to “pull down”

the known protein and any and all ligands and proteins that are attached to it. The proteins recovered can then be studied and applied to other various experiments. This, however, isn't always easy as custom antibodies are required for a specific protein. To circumvent this issue, the use of tags is most commonly instituted into the experimental design. The tag is introduced at either the N-terminus or the C-terminus of the protein of interest using one of the various cloning methods available. Antibodies specific for the tags can then be used instead of protein specific antibodies. The most common tags used in these type of experiments are those of higher sensitivity such as HA, GFP, flag, GST, etc (16). For testing the interaction of H-NOX with DGC we decided to tag H-NOX with flag and DGC with the HA tag.

Since our experimental design was based around using the native ribosome binding site and the cell's native transcriptional and translational machinery, we needed a strain of *S.woodyi* which lacked both proteins of interest. For our design we decided to use a knockout strain of *S.woodyi*, named *S.woodyi* Double Knockout (*S.woodyi* DKO) which was complemented using the *S.woodyi* wild type strain by Yueming Xu. This strain was confirmed, prior to us using it, via a genomic DNA PCR screen.

Unlike the many chemically made competent *Escherichia coli* (*E.coli*) cells that are commonly used in studies, *S.woodyi* is not a bacterial strain that has been made competent. Cell competency refers to a cell's ability to take up foreign molecules/DNA and storing that foreign matter for research purposes. In order to incorporate our constructs into the *S.woodyi* DKO strain, we needed to use a competent mediator strain which would hold the plasmid of interest and serve as a vector for introducing the plasmid into *S.woodyi* DKO by means of bacterial conjugation. The bacterial strain of choice was *E.coli* WM3064, an auxotroph strain of *E.coli* commonly used in experiments involving cell mating experiments. The reason we chose this

strain was due to its auxotrophic nature; *E.coli* WM3064 is incapable of synthesizing a chemical called diaminopimelic acid (DAP), which is a precursor for the amino acid lysine. Without this chemical, this strain of *E.coli* cannot grow. The nature of this bacterial strain is convenient with regards to conjugating (mating) experiments, since the removal of the chemical required for growth, from the growth medium, can easily eliminate the strain during the selection procedure for the complement(s) of interest.

The vector we chose to use is pBBR1MCS-2, a broad host range vector. Broad host range vectors differ from the general vectors for *E.coli* expression in a few ways. These vectors generally contain antibiotic genes for enzymes that are not secreted from the cell. In many cases this is essential for the process for selection for the mutant complements (17). These plasmids contain a conjugated helper plasmid which contains the mobilization and transmission genes required for conjugation and efficient replication in native bacteria (18).

2.3 Methods

2.3.1 Confirmation of the *S.woodyi* DKO strain

When dealing with native bacterial organisms such as *Shewanella woodyi* the occurrence of random mutations is possible. We decided to analyze the *S.woodyi* DKO strain before starting any additional experiments involving the use of this bacterium; a PCR screen of the *S.woodyi* DKO's genomic DNA would confirm whether or not the mutation was still intact. Since *S.woodyi* DKO possesses no antibiotic resistance of its own, we streaked out this strain from a glycerol stock on a Marine Media (MM) only agar plate containing no antibiotics. Likewise, as a positive control, *S.woodyi* wild type (WT) was streaked out on a MM only agar plate. These two plates were placed in a 28⁰C incubator and allowed to grow for 24 hours. One colony was picked

up from each respective plate and grown in 5ml of MM overnight at room temperature (25⁰C). These cultures were then used in the extraction of genomic DNA (gDNA) using the Zymo protocol for gDNA extraction. Following this, the concentration was taken via a UV Vis and observed to be about 160ng/ul for both the *S.woodyi* DKO and WT recovered gDNA. PCR reactions were set up using the Phusion (New England Biolabs) protocol using about 160ng of gDNA and 1μl of a 10mM stock of gene specific forward and reverse primers. Three reactions were set up using the DKO gDNA, the WT gDNA, and an empty pBBR1MCS-2 vector (negative control) for the purpose of amplifying the H-NOX, DGC, and H-NOX-DGC (whole operon) genes. The PCR conditions were set up according to the Phusion protocol. The PCR products were loaded onto a 1% agarose gel and run for 45 minutes at 120V. The gel was then visualized using a short-wave UV transilluminator (Figure 2-1)

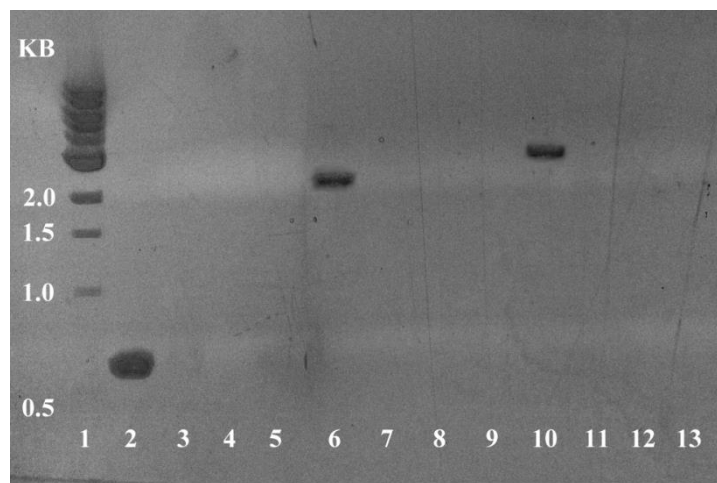


Figure 2-1. Agarose gel showing the results of the PCR screen of the *hnox* (lanes 2-5), *dgc* (lanes 6-9), and *hnox dgc* (lanes 10-13) genes from *S.woodyi* WT, *S.woodyi* DKO, and the pBBR1MCS-2 empty vector. The WT gDNA showed bands for all three genes (Lanes 2, 6, 10) while the empty vector (Lanes 3, 7, 11) and DKO gDNA (Lanes 5, 9, 13) showed an absence of bands for all three genes.

As expected, the PCR screen showed an amplification of *hnox* (~550bps), *dgc* (~1.6kbp), and the entire operon (~2.2kbp) for the WT strain of *S.woodyi*. These very same bands were not

observed for either the DKO strain or the empty pBBR1MCS-2 vector indicating that the PCR setup worked and confirmed the absence of both genes in the *S.woodyi* DKO strain.

2.3.2 Cloning/Site-Directed Mutagenesis

We decided to use pBBR1MCS-2 constructs that had been previously used in a phenotypic experiment. These constructs were: pBBR1MCS-2 *hnox* only, pBBR1MCS-2 *dgc* only, and pBBR1MCS-2 *hnox dgc*. Each of these constructs contained 26bp upstream of the target protein to ensure the presence of the genes' native ribosome binding site (rbs). We decided to choose these constructs for our study and use them as templates for generating the tagged equivalents (Figure 2-2).

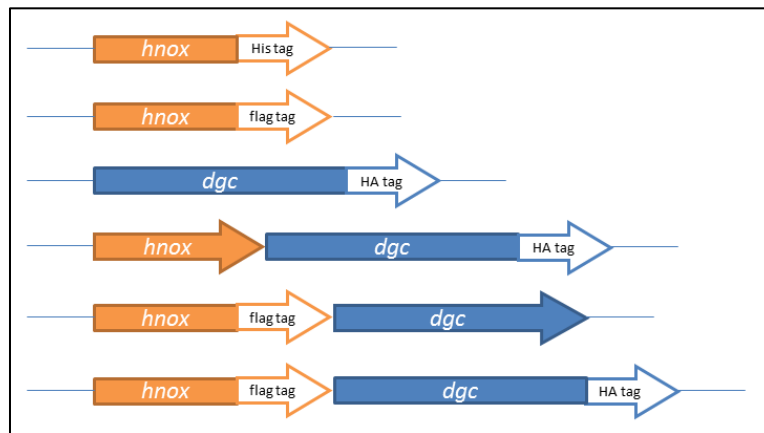


Figure 2-2. Constructs cloned for the purpose of *in vivo* expression and use in immunoprecipitation experiment.

Primers were ordered from the Stony Brook DNA Sequencing Facility for the purpose of introducing tags at the C-terminus of the respective genes via site-directed mutagenesis (Appendix). The Phusion protocol and reagents were used to set up the PCR reactions. The DNA templates, primers and expected products are shown in Table 2-1. A Biorad Thermocycler was used to run the reactions. The products were then digested using the DPN1 enzyme at 37⁰C for 3

hours to degrade any methylated DNA from the reactions. The DPN1 digested reactions were then transformed into DH5 α cells using a general lab protocol, plated on LB agar plates containing 10 μ g/ml of Kanamycin (Kan), and allowed to grow overnight. Colonies that grew on these plates were spotted on a different LB/Kan plate and screened using a colony PCR technique. The colonies were diluted in 50 μ l of autoclaved water and boiled at 95 $^{\circ}$ C to lyse the cells. 4.6 μ l of this mixture was then added to 5.4 μ l of goTaq solution (Promega) to make up the PCR reaction. The PCR conditions were set up according to the PCR protocol provided with the goTaq kit. The completed PCR reactions were then run on a 1% agarose gel and viewed on a shortwave transilluminator. Colonies which showed amplification at the correct size for their respective genes were grown overnight in 5ml of LB media. A plasmid DNA preparation kit (Zymo Research) was used to isolate and elute the plasmid DNA of the bacteria, which was then sent out for sequencing at the Stony Brook DNA sequencing facility in order to confirm the clones.

Template	Primers used	Product
pBBR1MCS-2 <i>hnox</i> only	QCCflagHNOX for & QCCflagHNOX rev	pBBR1MCS-2 <i>hnox</i> -flag
pBBR1MCS-2 <i>hnox dgc</i>	QC2flagHNOX for & QC2flagHNOX rev	pBBR1MCS-2 <i>hnox</i> -flag <i>dgc</i>
pBBR1MCS-2 <i>hnox</i> -flag <i>dgc</i>	QCDGCHA for & QCDGCHA rev	pBBR1MCS-2 <i>hnox</i> -flag <i>dgc</i> -HA
pBBR1MCS-2 <i>dgc</i> only	QCDGCHA for & QCDGCHA rev	pBBR1MCS-2 <i>dgc</i> -HA
pBBR1MCS-2 <i>hnox dgc</i>	QCDGCHA for & QCDGCHA rev	pBBR1MCS-2 <i>hnox dgc</i> -HA

Table 2-1. DNA templates, primers, and products of the site-directed mutagenesis reactions which were set up.

The *hnox* and *dgc* tagged constructs were to serve as the negative controls for the study, while the *hnox*-flag *dgc*, *hnox dgc*-HA constructs were the experimental constructs that would show if these two proteins are precipitated together. The final *hnox*-flag *dgc*-HA was included to confirm that the tags did not obstruct anything such as interference with the interaction of these two proteins. The *hnox*-His construct was made for convenience purposes; His tagged constructs are

common in our lab, therefore this construct would allow for an easy screening for the expression of the protein from *S.woodyi* DKO. The *hnox*-His construct was made via classical molecular cloning technique using the T7 Ligase system to ligate an empty pBBR1MCS-2 vector, digested with EcoRI-HF and XhoI, with an amplified and digested (with EcoRI-HF and XhoI) *hnox*-His insert. Both the digested vector and insert were purified from an agarose gel using a DNA gel recovery kit (Zymo Research) prior to setting up the ligation reaction. The ligase reaction was set up in accordance with the New England Biolabs protocol provided with the enzyme kit. The ligation reaction was incubated at room temperature (25⁰C) for one hour and then allowed further incubation at 16⁰C overnight. The finished reaction was transformed into DH5 α cells, plated on LB/Kan agar plates, and incubated overnight at 37⁰C. Any colonies that were observed on this plate were screened using the colony PCR method described previously. Positive colonies were grown overnight and used with the plasmid DNA isolation kit to elute the plasmid DNA. This DNA was then sent out for sequencing to confirm the clone.

Another clone was later made which involved expanding the 5' untranslated region (UTR) of the pBBR1MCS-2 *hnox*-His clone. We decided to increase the amount of base pairs preceding the H-NOX gene from 26 to 40 base pairs. The method we used here was a two-step site directed mutagenesis. This protocol was a combination of the two previously described cloning methods. We designed primers that contained one area which would anneal to the UTR section of interest and the other half of the primers contained a sequence which would anneal to the pBBR1MCS-2 vector. First these primers were used to amplify the UTR 40 bps upstream from the *hnox* gene using *S.woodyi* WT gDNA as the template. The amplified product was run on a 1% agarose gel and recovered using a DNA gel recovery kit. This product was then used as the primers for introducing the additional upstream base pairs to the pBBR1MCS-2 *hnox*-His

clone via PCR amplification using the Phusion protocol. The PCR products were digested with DPN1 and transformed and plated on LB/Kan agar plates. Any colonies that grew were plasmid prepped and sent out for sequencing to confirm the clone.

2.3.3 Complementation of the *S.woodyi* DKO with the pBBR1MCS-2 constructs

Unlike the many strains of *E.coli* that have been made chemically competent, *S.woodyi* is not capable of freely taking up and withholding foreign DNA. Due to this bacteria's nature, a donor strain had to be utilized to transfer the *hnox* and *dgc* genes into the *S.woodyi* DKO strain. The pBBR1MCS-2 constructs were transformed into the WM3064 strain of *E.coli*. The transformation protocol for this *E.coli* strain differs in two ways from the general transformation protocol. The heat shock step for WM3064 is 3 minutes instead of 43 seconds and the liquid media which is added to recover the cells, after the heat shock step, must contain 0.36mM DAP, otherwise the cells will not grow. The plates on which the cells are plated must also contain that same concentration of DAP. *S.woodyi* DKO and the transformed *E.coli* WM3064 were then inoculated in MM only and LB/Kan/DAP media at 25⁰C and 37⁰C overnight respectively. These two cell cultures were then streaked out, from liquid culture, on top of one another on a MM/LB/DAP agar plate. This plate was incubated at 28⁰C for an extended period of time (~36 hours) until both bacterial strains showed growth. *S.woodyi* can be distinguished from *E.coli* cells (white color) by its yellow/tan color. Any regions of the plate which contained a visual overlap of the two bacterial strains were picked up and streaked out onto MM agar plates containing 60µg/ml of Kan (6X Kan). These plates served to select for any *S.woodyi* DKO cells that successfully obtained the pBBR1MCS-2 *hnox*-His plasmid. Any colonies that grew on these plates were spotted on another MM/6X Kan agar plate and screened using the colony PCR method, using gene specific forward and reverse primers, described previously. These PCR

products were run on a 1% agarose gel and any colonies that showed a band at the respective gene size were grown up in 5ml of MM and used to make glycerol stocks (stored at -80°C). The *S.woodyi* DKO complements were confirmed via agarose gel electrophoresis.

2.3.4 Protein Expression and Detection

All experiments involving the pBBR1MCS-2 *hnox*-His construct were performed using the same protocol unless specified otherwise. Bacteria were grown overnight at their respective conditions. *E.coli* WM3064 was grown in LB media containing DAP. *S.woodyi* (both WT and DKO strains) was grown in MM. Kanamycin was added to the growth medium only if the bacterial strain was complemented with the plasmid (10µg/ml Kan for *E.coli* and 60µg/ml Kan for *S.woodyi*). The overnight cell cultures were diluted into fresh growth medium and allowed to grow until they reached an optical density (OD) of 0.6 measured at 600nm wavelength. 100µl of each culture was taken, pelleted and resuspended in 100µl of SDS buffer. Positive control samples were prepared by diluting the respective protein with a certain volume of water and adding SDS to this mixture. Samples were then boiled at 90°C for 5 minutes to lyse cells and prevent any protein aggregation. The boiled samples were spun down via a short spin in a mini-centrifuge and loaded onto an acrylamide gel.

Many different methods were attempted to detect the expression of the proteins from *S.woodyi* DKO. All of these methods involved the use of a western blot technique to determine if the cells were expressing the re-introduced proteins. To perform a western detection, the SDS lysate samples were run on an acrylamide protein gel at 130 volts and 400 milliamps for 65 minutes. Following the run, the western apparatus was prepared in the following fashion: foam layer, followed by a filter layer, followed by the gel, a nitrocellulose membrane is then carefully

placed upon the gel, followed by a filter layer, and finally another foam layer. This apparatus was then run in western transfer buffer at 40 volts and 400 milliamps for 2 hours in order to transfer all proteins from the gel to the nitrocellulose membrane. The membrane was blocked with 5% non-fat milk in TBST buffer for 1 hour to prevent non-specific interactions between the antibody and the membrane. The membrane was then blocked with 5% non-fat milk in TBST buffer with the addition of 1 μ l of the 6X His-HRP antibody for 1 hour prior to being washed with TBST buffer 5 times for 5 minutes each. The blot was then incubated for about 90 seconds with the Horseradish Peroxidase (HRP) substrate and placed in a western cassette for development in a dark room. The specific conditions for each western detection study will be briefly described in the results section.

2.3.5 RT PCR screen for mRNA

The strains which were to be used to extract total RNA from were grown in MM overnight at 25⁰C (complements strains had 60 μ g/ml of Kan added to their growth medium). 1ml of these cultures was used in the extraction of total RNA from the cells according to the Ambion RNA extraction kit protocol. The total RNA was then used in an RT PCR reaction set up in accordance to the Thermo Scientific RT cDNA PCR protocol.

2.3.6 Phenotypic Assays

Biofilm assays were performed by first streaking the strains on fresh plates and allowing them to incubate at 28⁰C for about 24 hours. Two colonies were inoculated per strain into MM (complement strains had 60 μ g/ml of Kan added as well) and allowed to grow overnight at 25⁰C. Media that had 100 μ M DPTA added to it was pre-decayed for 1 hour at room temperature prior to using it for dilutions. The cultures were diluted 100 fold into fresh MM. 100 μ l of the diluted cultures were plated into each well (10 wells per culture) in a 96 well plate. These plates also had

10 wells loaded with MM only (blanks) and 2 plates were set up per strain; one plate was used to read the OD of the cells and the other plate was used for Crystal Violet (CV) staining. The cells were allowed to grow statically at 25⁰C for about 20 hours. The bacteria in the OD plates were pipetted up and down several times and each well was transferred over to a sterile 96 well microtiter plate compatible with the microtiter plate reader. These plates were set aside while the CV plates were prepared. The CV plates were inverted and shaken to discard the media and any bacteria present in the media. The plates were then submerged in water several times and allowed to dry for about 20 minutes. 125µl of 0.1% Crystal Violet assay solution was loaded into wells containing biofilm residues. These plates were allowed to incubate for 30 minutes prior to discarding the CV and washing the wells several times with water. The wells were allowed 20 minutes to dry before 125µl of DMSO were added to each well and pipetted up and down to dissolve all the CV that was affixed to the biofilm. This solution was transferred to a sterile 96 well microtiter plate compatible with the microtiter plate reader. These plates were then inserted into the microtiter plate reader and scanned at a 570nm wavelength to determine the absorbance.

2.4 Results and Discussion

Since the 6X His antibody is readily available in our lab, we decided to first work with the pBBR1MCS-2 construct containing *hnox* with a C-terminal His tag. As a control experiment we decided to test if *E.coli* WM3064 is capable of expressing H-NOX via the pBBR1MCS-2 clone. The prediction for this study was that there would be no observed expression as there is a lack of homology between the structures of the ribosomes of *S.woodyi* and *E.coli*. We grew up the wild type WM3064, alongside the WM3064 complemented with the pBBR1MCS-2 *hnox*-His plasmid, as a negative control. A lab stock of a purified H-NOX protein with a C-terminal His

tag was used as a positive control for this test. 15µl of the two SDS samples and 1µl of the purified H-NOX were run on a 15% acrylamide gel and used for western detection (Figure 2-3)

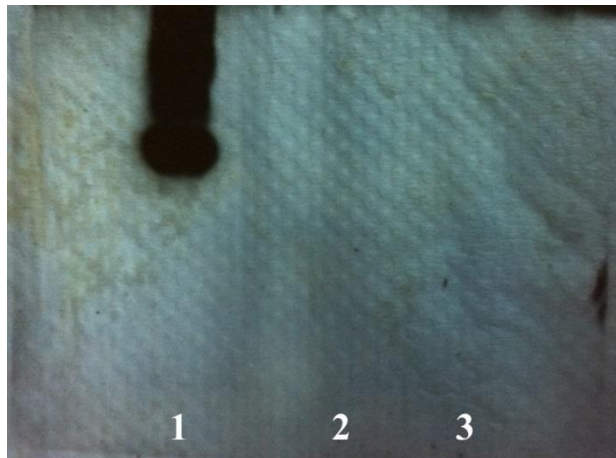


Figure 2-3. Developed western film showing the absence of a signal for both the WM3064 complement and the wild type WM3064 strain. Lane 1 contained the purified H-NOX control. Lane 2 contained lysate from the WM3064 pBBR1MCS-2 *hnox*-His complement and lane 3 contained lysate from WM3064 WT. The positive H-NOX control was observed to be very concentrated as seen by the partial bleaching effect.

As expected, the WM3064 strain was unable to express this protein as its ribosomes were most likely not able to recognize and bind to the rbs sequence specific to the *S.woodyi* strain.

We decided to follow up this study by performing an identical setup using the *S.woodyi* DKO pBBR1MCS-2 *hnox*-His complement. We grew four of the *S.woodyi* DKO colonies, which screened positive for the pBBR1MCS-2 *hnox*-His clone, overnight at 25⁰C in MM/6X Kan. The *S.woodyi* DKO strain was also grown overnight in MM only at 25⁰C as a negative control. The SDS samples were prepared as previously described and 15µl of each of the SDS pellet samples and 0.5µl of the purified H-NOX were loaded onto a 15% acrylamide gel and later used for western detection (Figure 2-4).



Figure 2-4. Western film showing the absence of a signal for H-NOX from the *S.woodyi* complements. Lane 1 was loaded with a NEB 230 kDa prestained marker. Lanes 3 & 4 were loaded with lysate from *S.woodyi* WT and *S.woodyi* DKO respectively (negative controls). Lanes 5 – 8 were loaded with lysate from the 4 different *S.woodyi* DKO complements. Lane 10 was loaded with purified H-NOX protein.

From the western results we observed no signal corresponding to the H-NOX protein. From this study we decided that a small scale study was giving an insufficient amount of protein for the purpose of detection via the 6X His antibody. We decided to perform two tests: one using a larger pellet volume and another test to observe the lowest concentration of protein that is detectable by the 6X His antibody.

We measured the concentration of the H-NOX His purified protein using a Bradford Assay protocol. Several SDS samples were prepared with decreasing concentrations starting from 500ng of protein down to a mere 6.25ng of protein. These samples were run on a 15% acrylamide gel and used for running a western (Figure 2-5).

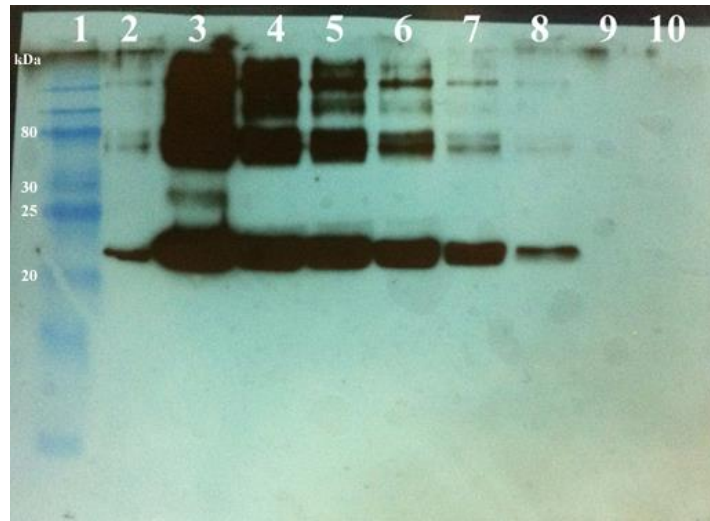


Figure 2-5. Western showing our analysis of the sensitivity of the 6X His antibody using a purified H-NOX protein with known concentration. Lane 1 was loaded with a NEB 230 kDa prestained marker. Lane 2 contained bleedover from lane 3. Lanes 3 – 8 were loaded with 500ng, 100ng, 50ng, 25ng, 12.5ng, and 6.25ng of purified H-NOX protein respectively.

From this study we determined that the 6X His antibody sensitivity is able to detect protein concentrations which go even below 6.25ng. Dividing this result by the molecular weight of the protein (~20.8 kDa) shows us that the molar sensitivity is on the order of approximately 300nM concentration for the H-NOX protein. Knowing this we decided to repeat the detection of H-NOX from the *S.woodyi* DKO complement by changing up several variables and increasing the volume of the starting culture.

An overnight culture of *S.woodyi* DKO and *S.woodyi* DKO pBBR1MCS-2 *hnox*-His were grown over night in 5ml of MM and MM/6X Kan respectively. These cultures were diluted in 100ml of fresh MM and MM/6X Kan and allowed to reach an OD of 0.8. At this point the cells were pelleted at 5,000 rpm for 15 minutes at 4⁰C. The cells were then resuspended in 5ml of PBS buffer containing 1mM PMSF and 5mM BME and lysed using a hand sonicator. The crude lysate was then centrifuged at 18,000 rpm for 1 hour at 4⁰C. The cleared lysate was incubated with 100μl of Ni NTA beads for 1 hour. The lysate was carefully pipetted out and 100μl of SDS were added to these beads to resuspend them. The beads were boiled at 90⁰C and

15 μ l of the SDS buffer were loaded onto a 15% acrylamide gel. Some of the cell debris was also resuspended in SDS and boiled before being loaded onto the gel. This gel was then used for western detection (Figure 2-6).

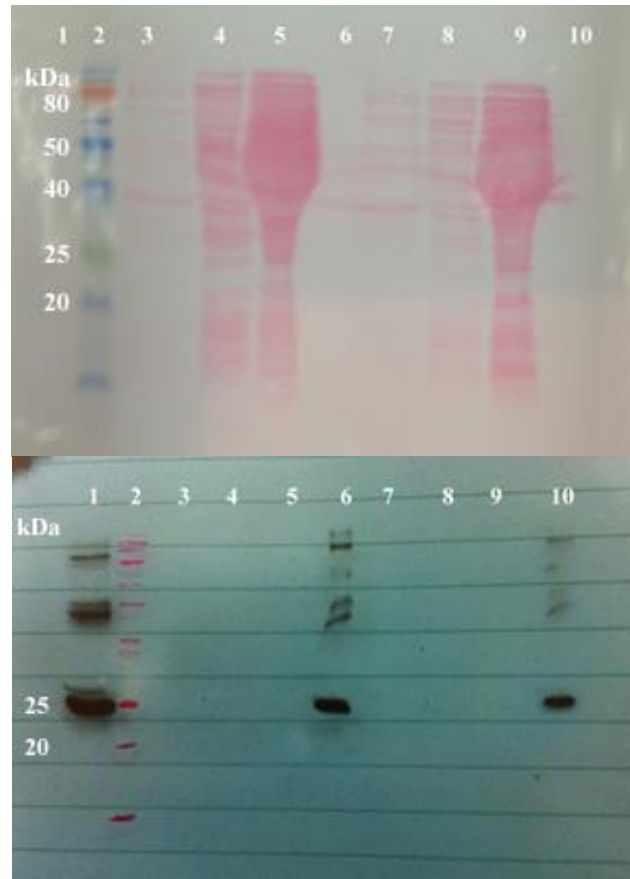


Figure 2-6. (Top) A Ponceau staining of the transferred western blot, showing the protein distribution of each sample loaded. (Bottom) Developed western film for the detection of H-NOX from *S.woodyi* DKO complement using 6X His antibody. (Both) Lanes 1, 6, and 10 contained 25ng, 12.5ng, and 6.25ng of purified H-NOX respectively. Lane 2 contained 230 kDa prestained protein marker (NEB). Lanes 3 – 5 were loaded with *S.woodyi* DKO pellet, lysate, and Ni NTA beads respectively. Lanes 7 – 9 were loaded with *S.woodyi* DKO pBBR1MCS-2 H-NOX His pellet, lysate, and Ni NTA beads.

The result still came up negative at this point, leading us to consider that maybe we were catching the cells at an OD that did not correspond to the middle/late log phase of the *S.woodyi* bacterial strain. Moreover we decided to try growing these cells in the presence of Nitric Oxide to see if this chemical perhaps stimulates the transcription and subsequent translation of the complemented gene. We decided to perform a growth curve (one including NO in the growth

medium and one without NO) for both the *S.woodyi* DKO and the *S.woodyi* DKO pBBR1MCS-2 *hnox*-His. An overnight culture of both strains was diluted into 50ml fresh media. An initial time point OD was taken and an additional time point OD was taken about every hour following this for a total of 10 hours. Afterwards the cultures were allowed to grow overnight and a final OD was taken the next day (Figures 2-7, 2-8).

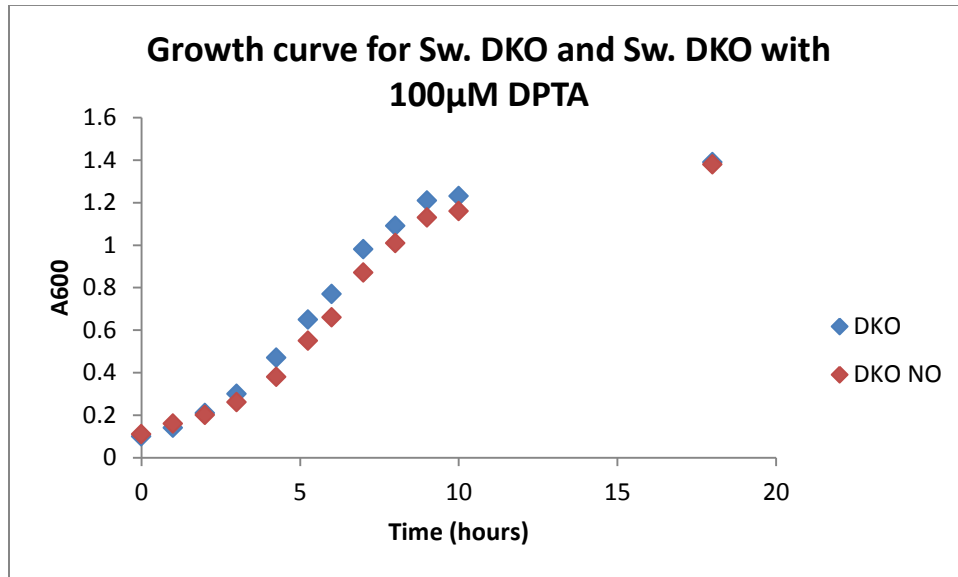


Figure 2-7. Growth curve comparison for *S.woodyi* DKO grown in MM and MM containing 100µM DPTA. Time points were taken for 10 hours and a final time point at 18 hours of culture growth.

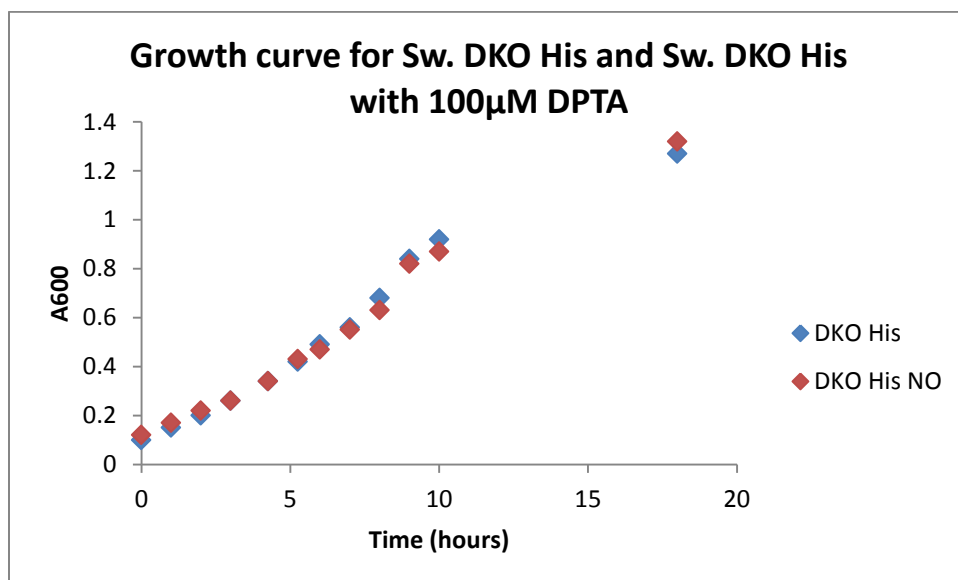


Figure 2-8. Growth curve comparison for *S.woodyi* DKO pBBR1MCS-2 *hnox*-His grown in MM/6X Kan and MM/6X Kan containing 100 μ M DPTA. Time points were taken for 10 hours and a final time point at 18 hours of culture growth.

These growth curves provided us with 2 aspects of information: the log and late log growth curve for *S.woodyi* is very similar to that of *E.coli* and also that the addition of NO to the growth medium (pre-decaying of the NO was not performed during this experiment) did not affect the growth rate of these cells to any significant extent. One observation that we found interesting was the shape of the growth curve of the *S.woodyi* DKO complement. The growth curve was found to be more linear than the commonly observed sigmoidal curve. This may be due to the high concentration of antibiotic in the growth medium; this may possibly slow down the cellular replication machinery while the cells increase other biological pathways to compensate for the higher concentration of Kanamycin. However due to the absence of the time points after the 10th hour it is hard to make clear conclusions as to whether there actually is a difference between the growth behavior between the *S.woodyi* DKO strain and the complement strains as the possibility exists that the missing time points could add up to a sigmoidal behavior.

During the growth curve experiment, we pelleted 200 μ l at every time point for the purpose of using these samples to see if perhaps the cells express the protein under growth conditions involving NO. Points from the middle of log phase, late log phase, and stationary phase were used to run a protein gel which was used for a western transfer (Figure 2-9).

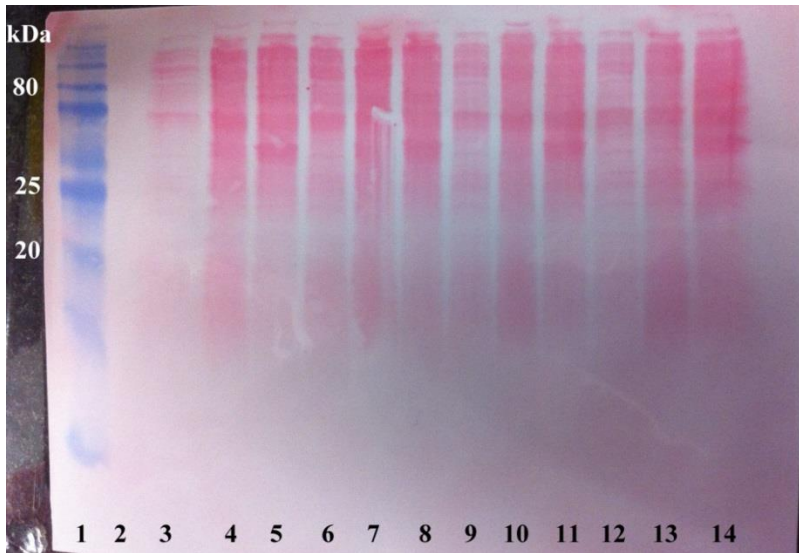


Figure 2-9. Ponceau stained blot showing bound proteins from the cell lysate from 12 different growth curve samples. Lane 1 was loaded with a 230 kDa prestained marker (NEB). Lane 2 was loaded with 6.25ng of purified H-NOX protein. Lanes 3 – 5, 6 – 8, 9 – 11, 12 -14 contained samples from mid log phase, late log phase, and stationary phase from *S.woodyi* DKO, *S.woodyi* DKO with NO, *S.woodyi* DKO *hnox*-His, and *S.woodyi* DKO *hnox*-His NO respectively.

The western for this experiment (not shown) also did not show any signal bands corresponding to the H-NOX protein weight.

During the growth curve experiment we decided to take an aliquot of cells from the time point which gave an OD close to 0.8. We diluted these cells 1 million-fold and plated 100µl on six MM agar plates. We decided to use these plates to count the number of cells that were present at an OD of 0.8, and determine the number of bacterial cells that would be required to provide a protein concentration in the range of 6.25ng. The amount of colonies observed on those plates was: 154, 164, 198, 217, 223, and 298 (Average: 209). Multiplying this by the dilution factor gives $2.09 * 10^8$ *S.woodyi* DKO cells per 100µl of cell culture at an OD of 0.8.

$$\text{Lowest concentration of His detectable by 6X His antibody: } \frac{6.25 * 10^{-9} \text{ g}}{20,800 \frac{\text{g}}{\text{mol}}} = 3.005 * 10^{-13} \text{ mol}$$

$$\text{Molecules of H – NOX: } 3.005 * 10^{-13} \text{ mol} * 6.022 * 10^{23} = 1.81 * 10^{11} \text{ molecules}$$

If we make a minimal assumption that each cell generates 1 copy of the protein then theoretically 1ml of cell culture at an OD of 0.8 (2.09×10^{11} cells) should be sufficient to lead to signal detection via a western development.

At this point we tried two additional experiments: extending the UTR upstream of the H-NOX His construct and detection of H-NOX from *S.woodyi* DKO pBBR1MCS-2 *hnox*-flag using M2 flag antibody. We decided to extend the UTR of the pBBR1MCS-2 *hnox*-His construct after coming across a paper which talked about incorporating up to 38 bps upstream of the gene to circumvent their protein expression problem. We cloned an additional pBBR1MCS-2 construct containing 40 bps upstream of the *hnox* gene with a C-terminal His tag (19). We mated and tried expressing this protein from a culture of 100ml at an OD of 0.8. Using the same methods as previously described we ran the respective samples on a gel and transferred them onto a nitrocellulose membrane. The developed western from this experiment demonstrated the same absence of a signal as the previous times (data not shown). We followed up this experiment with an anti-flag detection of HNOX from *S.woodyi* DKO pBBR1MCS-2 *hnox*-flag complement. Antibodies specific for tags used in sensitive experiments such as immunoprecipitation are more sensitive and therefore can be used to detect protein concentrations on the Pico molar scale. The protocol for the flag experiment was done exactly as the western protocol for the His tagged experiments using 100ml cell culture and the M2 flag antibody which we borrowed from the Carrico Lab. The results for the western are depicted in figure 2-10.

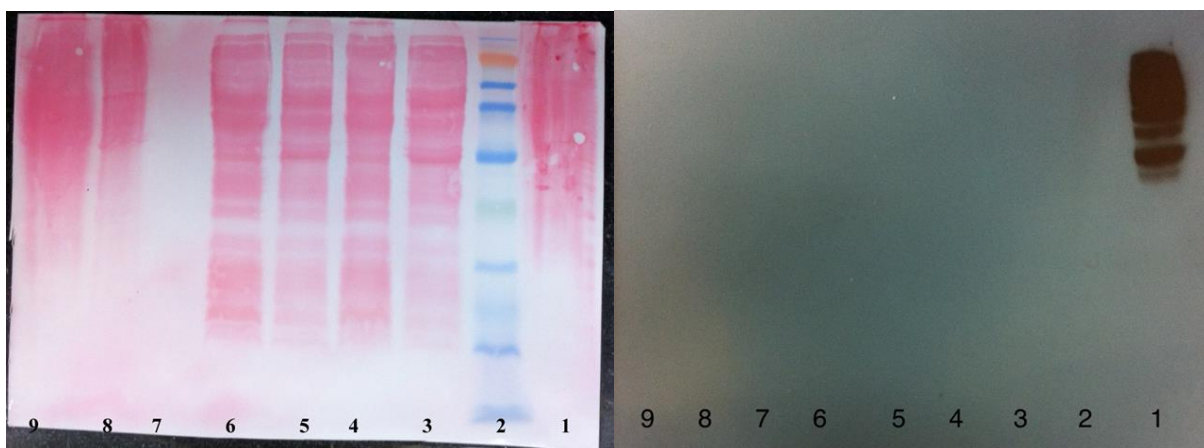


Figure 2-10. Ponceau stained blot (Left) and the developed western film (Right) for the detection of H-NOX from *S.woodyi* DKO pBBR1MCS-2 *hnox*-flag using the M2 flag antibody. Lane 1 was loaded with mammalian cell lysate (positive control). Lane 2 was loaded with 230 kDa prestained protein marker (NEB). Lanes 3 and 4 were loaded with *S.woodyi* DKO lysate from cells at an OD of 0.8 and stationary phase respectively. Lanes 5 and 6 were loaded with *S.woodyi* DKO pBBR1MCS-2 *hnox*-flag lysate from cells at on OD of 0.8 and stationary phase respectively. Lanes 8 and 9 were loaded with *S.woodyi* DKO pellet and *S.woodyi* DKO pBBR1MCS-2 *hnox*-flag pellet respectively.

After observing an absence of a signal for H-NOX even after the incorporation of a more sensitive antibody we chose to perform an RT PCR to confirm if the cells contain presence of the mRNA for the H-NOX protein. This technique tests to see if the transcription of the protein is being executed by the cells. We extracted the total RNA from *S.woodyi* WT, *S.woodyi* DKO, *S.woodyi* DKO pBBR1MCS-2 *hnox*-His, and *S.woodyi* DKO pBBR1MCS-2 *hnox*-flag *dgc*-HA cell strains. Total RNA extracted was then used to synthesize cDNA using reverse-transcriptase. The obtained cDNA was then screened via a PCR reaction, using gene specific forward and reverse primers, to test for the presence of the *hnox* gene. A lab stock of *S.woodyi* WT gDNA was used as an additional positive control for this test. These samples were run on a 1% agarose gel (Figure 2-11).

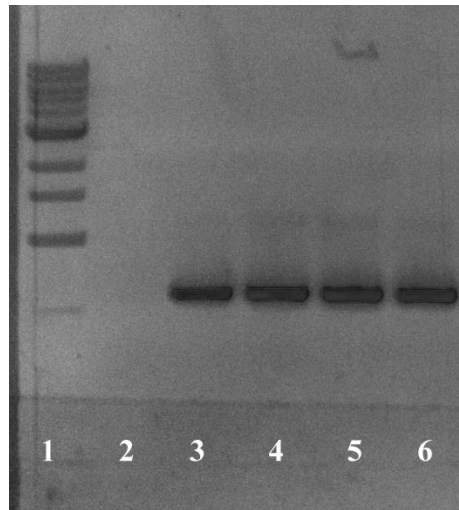


Figure 2-11. Agarose gel showing amplification of cDNA using gene-specific forward and reverse primers for the *hnox* gene. Lane 1 was loaded with 1kb DNA ladder (NEB), lane 2 was loaded with cDNA from *S.woodyi* DKO, lane 3 contained the cDNA from *S.woodyi* WT, lane 4 was the positive control using *S.woodyi* WT gDNA as a template for the PCR screen, lanes 5 and 6 contained cDNA from *S.woodyi* DKO pBBR1MCS-2 *hnox*-His and *S.woodyi* DKO pBBR1MCS-2 *hnox*-flag *dgc*-HA complements respectively.

Data from this test indicated that the gene was being transcribed. It is unknown as to what extent the transcription was taking place, however this told us that the problem for the lack of expression did not exist at the step of transcription. We decided to perform two sequential experiments involving analysis of the morphology of the bacterial cell colonies and an analysis of phenotypic characteristics of *S.woodyi* WT, *S.woodyi* DKO, *S.woodyi* $\Delta hnox$, and all the *S.woodyi* DKO complements with we have confirmed. Morphology was observed by plating and growing the bacteria on agar plates containing their respective growth conditions. Ideally, any bacterium that does not contain *dgc* should show a more “wrinkled” morphology then smooth. All the strains we grew up on agar plates showed a smooth texture. This was not surprising as most carefully performed morphology experiments utilize powerful microscopic machinery to view morphologic changes and differences using large magnifications. We decided to take the colonies on these plates and use them to perform a phenotypic assay. In this case we used a dye

called crystal violet dye (CV) that is capable of binding to affixed cells. We grew up *S.woodyi* WT, *S.woodyi* DKO, *S.woodyi* $\Delta hnox$, and all the *S.woodyi* DKO complements in their respective growth media and followed the protocol described previously in the methods section. To graph this data we took the average CV and divided it by the average OD of that particular strain (Figure 2-12).

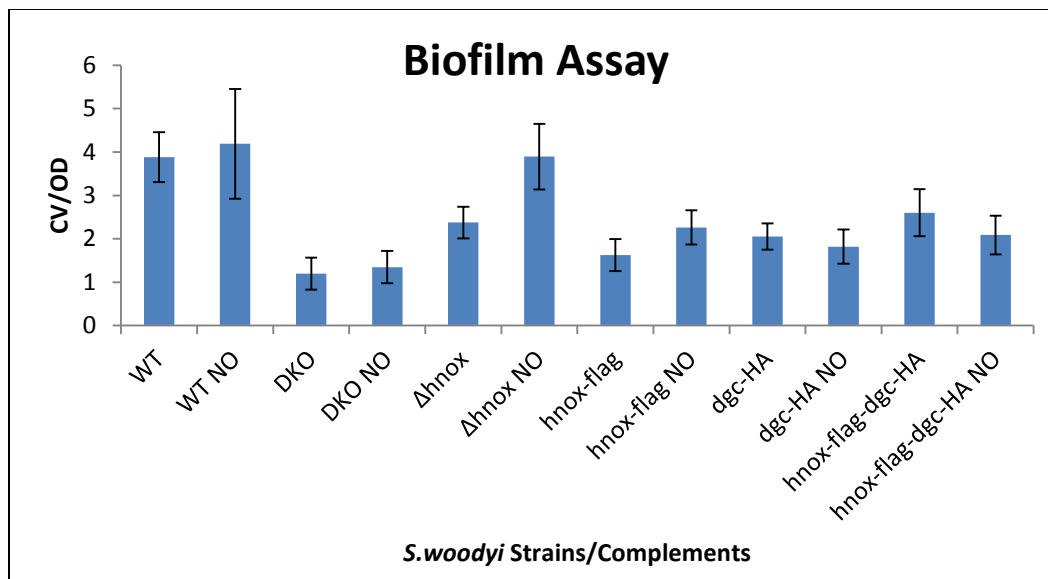


Figure 2-12. Bar graph showing the CV/OD measurement for the various *S.woodyi* strains with and without NO. Error bars represent one standard deviation of uncertainty for each strain. This study was performed as a duplicate.

This biofilm assay provided us with several key points of insight. Aside from the error bars for the WT NO and *hnox-flag-dgc-HA*, all other error bars are small and thus acceptable. Since NO promotes cell motility, strains grown in the presence of NO should exhibit a lower CV/OD ratio compared to the strains grown in the absence of NO. For the WT, it is hard to tell from this study as the error bars for the NO strain are very high. The DKO strain showed little difference between the cells grown with NO and those without it. This makes sense due to the fact that neither of the genes encoding for the H-NOX and DGC proteins are present, so the

observed state of cellular motility should be similar for both of these samples. As such, there is no significant difference between the CV/OD ratios for the DKO and DKO NO samples. The error bars for these two samples also do overlap showing that this seems to be the case. The results for the *Δhnox* strains are hard to explain. In the absence of H-NOX, DGC should be able to keep its cyclase activity dominant and promote a sessile cell state. There should be no difference in the CV/OD ratios for this pair of samples. The fact that the error bars don't overlap indicates that the study for this strain would have to be repeated in order to obtain more accurate results. Although the complements were confirmed via a PCR screen, this data implies that the expression of the respective proteins may be too low to observe any phenotypic characteristics which may have otherwise been exhibited if there was significant protein expression; the CV/OD ratios for the complements are not that much different when compared to the CV/OD ratios for the DKO strain. The error bars do overlap to a significant extent, thus the data represented by the CV/OD ratios of the complements is difficult to explain. For the *hnox*-flag and *dgc*-HA complements there shouldn't be much difference in their phenotypic ratios. For the complement containing both tagged proteins, there is a slight decrease in the formation of biofilm from the cells grown in media containing NO, however since the error bars overlap this study would need to be repeated in order to confirm this observation.

A final experiment was performed to see how efficiently the plasmid is replicated within the *S.woodyi* system. We inoculated one colony from one of the complement strains plates used for the biofilm assay and allowed it to grow overnight. We used a plasmid prep kit (Zymo research) to extract plasmid DNA from the *S.woodyi* complement culture. When we took a reading on the UV-vis we observed nothing out of ordinary. However, when we transformed this extracted plasmid into DH5 α cells and plated the cells on agar plates, we only observed 5 – 6

colonies; the lab stock of DH5 α cell is very competent, usually giving a lawn of cells if the entire volume of recovered cells is plated on one plate. This was repeated again for consistency and we observed the same results. This fact may indicate that the plasmid isn't replicated and transferred on at a frequency high enough for every cell to contain at least one copy of the clone. Another explanation is that the *S.woodyi* cells possibly degrade this plasmid after a certain amount of time (perhaps after the cells randomly mutate and adapt a resistance to the Kanamycin in the environment). There is no absolute reason that we can provide to this phenomenon, however it is clear that this may be the cause of the under-expression or even lack of expression of the complemented proteins. It may be possible to circumvent this problem by using an overexpression method rather than relying on native sequences specific to the species.

Chapter 3: Analysis of the Interaction of isolated DGC motifs with HNOX using Analytical Ultracentrifugation

3.1 Abstract

The study of protein interactions in molecular science holds a wide range of significance. By studying and understanding the mechanism that a protein uses to interact with and affect other molecules and proteins, it becomes possible to use modern day research methods to find ways to manipulate the protein of interest. Di- guanylate cyclase (DGC) is an example of a protein complex that holds an important role in the regulation of the synthesis and breakdown of c-di-GMP. C-di-GMP is a second messenger molecule that has been shown to play an active role in regulating the motile state in bacteria. By studying the EAL, PAS, and GGDEF domains of DGC, we hope to gain a further understanding of how each individual protein contributes to the overall functionality of the complex. The goal of this study was to analyze the behavior of each of these three proteins in the absence of the other two proteins. Current analytical ultracentrifugation data demonstrates the oligomeric states for the EAL only, EAL with H-NOX, and PAS only follow the oligomeric states observed during the pull down assay studies done in a previous experiment. The activity assays performed imply EAL and GGDEF possess a dependence on the other two proteins and/or native biological environment for their enzymatic activity. Further studies will be performed to observe the oligomeric states for PAS with H-NOX, GGDEF only, and GGDEF using Analytical Ultracentrifugation.

3.2 Introduction

DGC is a large protein which has been shown, using *in vitro* studies, to directly interact with the H-NOX protein. The association of these two proteins allows for the regulation of c-di-GMP levels in the cell. Since c-di-GMP has been observed to affect the formation of biofilm in

bacteria, the interaction of H-NOX with DGC is very significant and studying this interaction may lead to further insight on possible ways to manipulate the key details of their interaction.

DGC contains three important domains: EAL, PAS, and GGDEF. Two of these domains (GGDEF and EAL) give DGC its cyclase and phosphodiesterase activities respectively, while the other (PAS) functions as a protein that facilitates DGC's interaction between its own motifs and with other proteins.

Activity assays can tell a lot about the protein of interest. In this case EAL and GGDEF are both functional domains when part of the DGC complex. However, it isn't known if these domains are able to retain their activity when isolated from the complex. The activity assays performed serve the very purpose of showing if these motifs are independent of other interactions for their own enzymatic activity.

An Analytical Ultracentrifuge is a centrifuge which uses optical detection machinery and allows for accurate and real-time observation of molecular sedimentation within the rotor cells (20). This centrifuge is optimized for very high speeds for the purpose of covering an enormous protein range from very small molecule (high speeds) to extremely large protein complexes (low speeds). It is also capable of scanning using UV range wavelengths as well as wavelengths above 400nm. The experiments performed in this project were of the Equilibrium type, which means that we were interested in the final steady-state of our proteins.

3.3 Methods

3.3.1 Protein Purification

The constructs for the three proteins were all made in the pET 20b vector by Sajjad Hossain (Appendix). All three constructs were transformed into BL21 cells and plated on LB agar plates containing 10 μ g/ml of both Ampicillin (Amp) and Chloramphenicol (Cam). A colony

from each plate was inoculated and grown overnight in 5 ml of LB/Amp/Cam. The overnight culture was then diluted into 1 liter of 2XYT media and allowed to grow at 37°C to an OD of 0.8 before being induced with 100µM of IPTG. The induced culture was allowed to incubate at 16°C overnight for about 14 hours. These cells were pelleted using a centrifuge at 5,000 rpm for 15 minutes at 4°C. Following this the cells were resuspended in Buffer containing 250mM NaCl, 50mM Tris, 25mM KCl, 10mM MgCl₂, 500µM EDTA, 1mM PMSF, 5mM BME, and 0.1M Glycerol, pH 8. The cells were lysed using a sonicator after which the lysate was centrifuged at 18,000 rpm for 1 hour at 4°C in order to remove all the cell debris and membranes from the lysate. The cleared lysate was run over 1ml of Ni NTA agarose beads which were equilibrated with the lysate buffer. Four washes of 25ml of 10mM imidazole, 25ml of 20mM imidazole, 10ml of 50mM imidazole, and 5ml of 100mM imidazole were performed on the beads in order to elute any and all bacterial proteins and proteins that were weakly bound to the Nickel beads. The proteins were eluted using 10ml of 250mM imidazole and injected onto the Fast Protein Liquid Chromatography (FPLC) system for further purification. Purification using the FPLC was done using a superdex200 column (60/16). Proteins were injected onto the column and run at a flow rate of 1ml/minute using a filtered buffer containing 250mM NaCl, 50mM Tris, 25mM KCl, 10mM MgCl₂, 500µM EDTA, and 5mM BME, pH 8. Proteins were collected based on the peaks outputted by the UV lamp. 10% glycerol was added to the proteins prior to storing them at -80°C.

3.3.2 Analytical Ultracentrifugation (AUC)

Two types of reactions were set up using the AUC: one type involved only the protein by itself, the other type involved the addition of H-NOX to the protein sample.

Reactions without H-NOX involved loading the protein into the cell at varying concentrations. Generally, a molar concentration of 4 μ M or higher gave data that was consistent and easy to fit. The three speeds, for each run, were calculated according to the formulas:

$$\sqrt{\left(\frac{100}{MW}\right)} * 8,000 \quad \sqrt{\left(\frac{100}{MW}\right)} * 12,000 \quad \sqrt{\left(\frac{100}{MW}\right)} * 15,000$$

where “MW” is equal to the molecular weight of the protein in kilo Daltons (20).

Reactions with H-NOX involved first preparing an H-NOX NO complex. This preparation was done inside of a glove bag to prevent oxidation of the heme iron of H-NOX. 28mg of dithionite (reducing agent) were dissolved in 500 μ l of H-NOX buffer. 40 μ l of dithionite was added directly to 400 μ l of purified H-NOX, and incubated for 15 minutes, in order to reduce the heme iron to its ferrus state. The reduced H-NOX was confirmed on the UV-vis by the presence of a soret band at 425nm. 300 μ l of this reduced H-NOX was desalted using a Pd-10 desalting column in order to remove dithionite from the solution (dithionite can react with NO). 30 μ l of 50 μ M DEA were added to the desalted H-NOX and incubated for 30 minutes. The NO bound H-NOX was confirmed on the UV-vis by the presence of a soret band at 403nm. The concentrations of the DGC domain protein, H-NOX Fe⁺², and H-NOX Fe⁺² NO were measured using a Bradford Assay. The ratios were then set up such that the DGC domain protein’s molar concentration was higher than that of the molar concentration of H-NOX.

The data obtained from the AUC was fitted using software called Heteroanalysis. The density and Vbar for the individual proteins were calculated using a program called Sednterp.

3.3 Results and Discussion

The construct we decided to use for this experiment were ones that have been used in a previous pull down study. As such, the circular dichroism data for these three proteins was already known to us (Figure 3-1) (15).

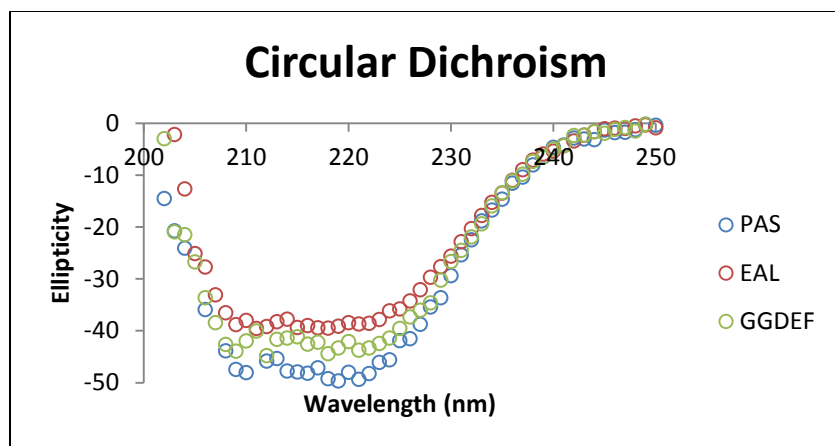


Figure 3-1. Data from the circular dichroism study indicating the presence of secondary structure elements in each of the three proteins. Data adopted from Sajjad Hossain.

From the circular dichroism study we observed that all three proteins showed a broad curve implying a helical structure. This suggested that the proteins we were purifying and working with were in fact folded.

We decided to start this project by optimizing the purification conditions for the EAL domain of DGC. Initially, we chose to use TB media as the induction media since it's a very rich media that has been optimized for *E.coli* growth. One problem that we ran into with using TB media is that under these induction conditions, a protein of similar molecular weight to that of EAL (30.5 kDa) was being co-expressed and subsequently co-purified with Ni NTA affinity chromatography (data not shown). Even more surprisingly, this protein co-purified via the FPLC, indicating that the superdex200 column was not able to distinguish the difference in molecular weight between these two proteins and thus separate them efficiently. We decided to use 2XYT as our induction condition and this seemed to eliminate the expression of the other protein. A western was also performed to confirm the EAL protein (Figure 3-2).

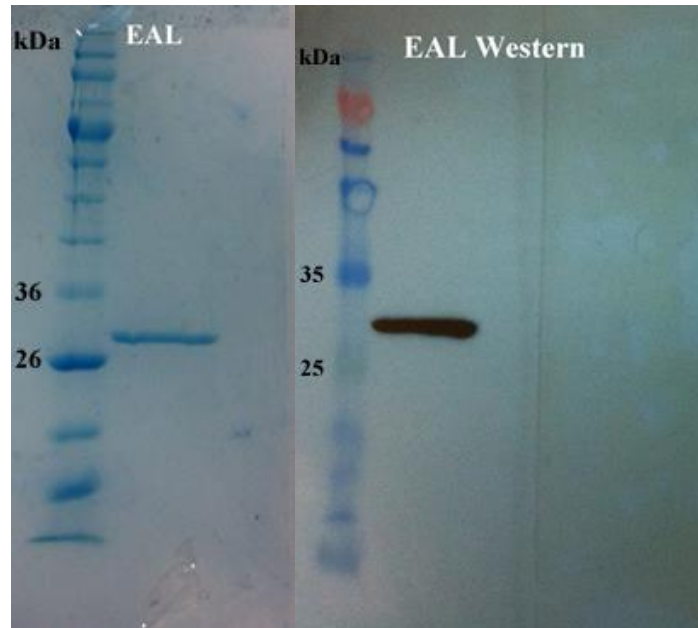


Figure 3-2. (Left) Coomassie Blue stained gel (Right) developed western blot showing an FPLC purified EAL band.

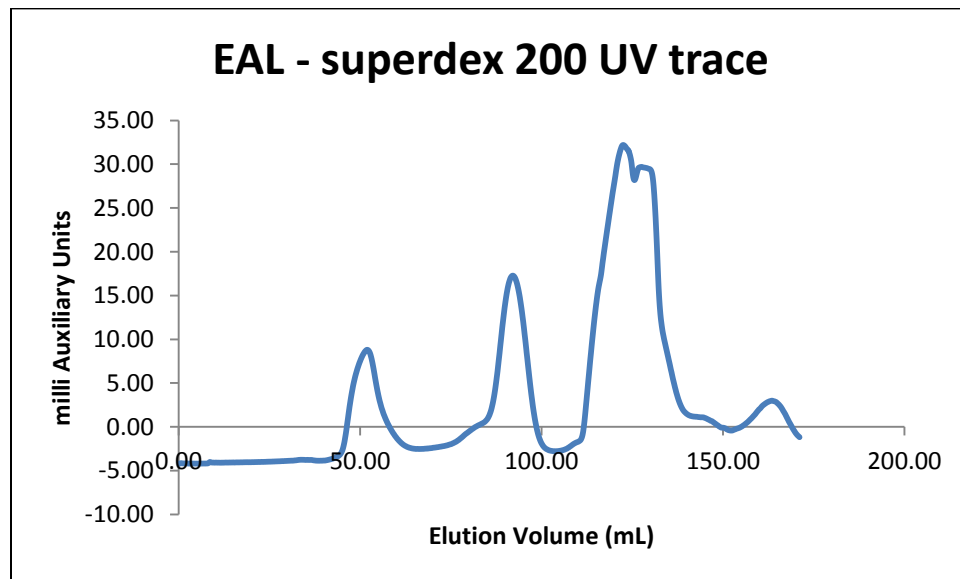


Figure 3-3. UV trace of the EAL profile using the FPLC system. Peak at 90ml corresponds to folded EAL protein.

After purifying 6 liters of EAL pellet we obtained a sufficient concentration of 7.5 μ M. We used this protein to run an activity assay to see if EAL was active in the absence of the other 2 domains. We also used this EAL to set up a sedimentation equilibrium AUC run (Figure 3-4).

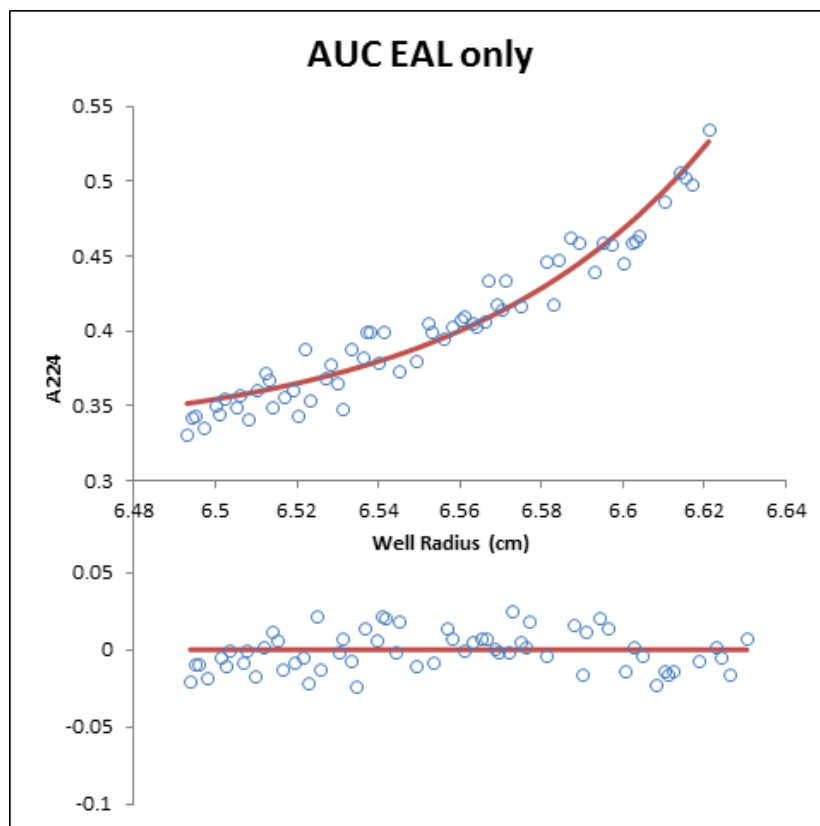


Figure 3-4. Example of a graph for EAL outputted from Heteroanalysis. The fit of all the graphes gives a molecular weight corresponding to 61,008 Da for EAL.

The AUC data for the EAL by itself shows that it exists in a dimer with itself in the final steady-state of the run.

We followed up this run by loading EAL with H-NOX using the method previously described. We set up samples with both the ferrus H-NOX and ferrus H-NOX bound to NO. The EAL which was set up with NO bound HNOX showed a molecular weight corresponding to a EAL-HNOX-EAL-HNOX complex (dimer-dimer complex) (Figure 3-5).

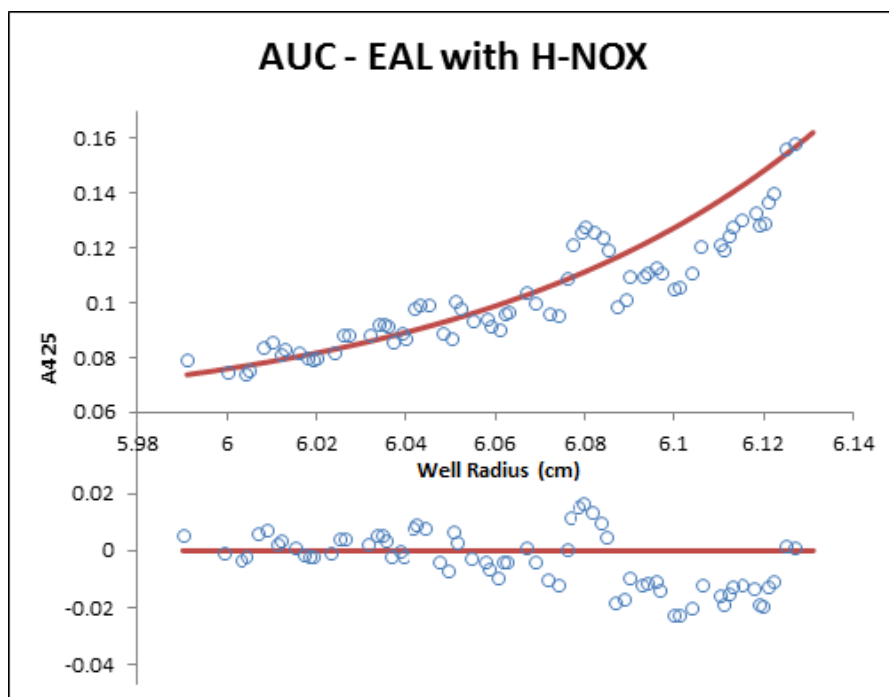


Figure 3-5. Example of a graph outputted by the AUC. The reported molecular weight of final steady-state of the equilibrium run was reported to be around 101,597 Da. This MW implied a EAL-HNOX-EAL-HNOX complex.

We set up an assay for the analysis of EAL activity in its isolated stated. The enzyme was incubated with substrate (c-di-GMP) for 30 minutes prior to quenching the reaction by boiling the sample for 5 minutes at 90⁰C. The reaction was run on the HPLC along with the pGpG and c-di-GMP standards. The graph points were exported and overlaid using excel (Figure 3-6).

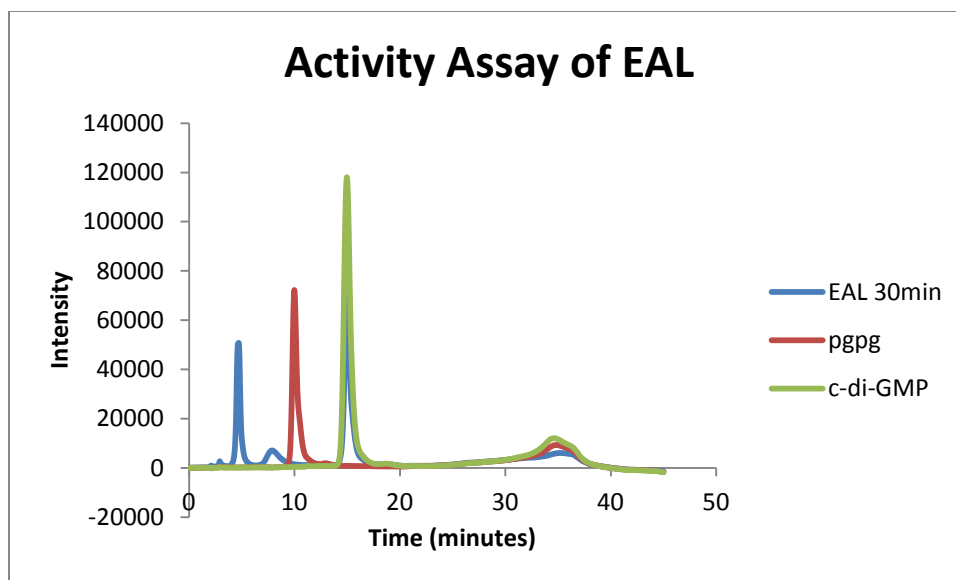


Figure 3-6. An overlay of the c-di-GMP and pGpG standards along with EAL incubated with c-di-GMP for 30 minutes on the HPLC.

The presence of an unexpected peak was observed to be eluted at 5 minutes into the run. It is difficult to assess what this chemical species might be based on the standards that were run. It is very possible that this peak may be enzyme debris from when the reaction was quenched, however, without performing additional tests such as mass spectroscopy, for example, it is impossible to draw any strong conclusions as to the identity of this chemical species. However, activity-wise, from the overlay, we see that the c-di-GMP was not degraded to any extent by the enzyme and that there is no indication of a pGpG peak in the EAL reaction. From this we can conclude that the isolated EAL domain cannot maintain its activity on its own.

We purified PAS in the same manner that we had purified EAL. Although the protein yield was lower than for the EAL protein (Figure 3.7), PAS is a protein which does not have enzymatic activity of its own therefore we were able to concentrate this protein without it precipitating out of solution. A western was run for the peak at 100ml to confirm the PAS protein (Figure 3-8).

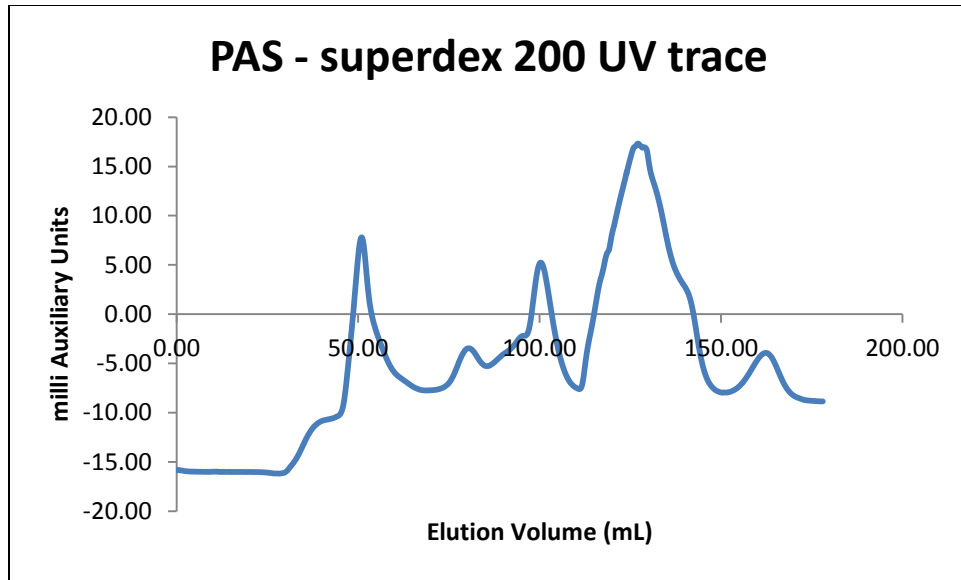


Figure 3-7. UV trace of the PAS profile using the FPLC system. Peak at 100ml corresponds to folded PAS protein.

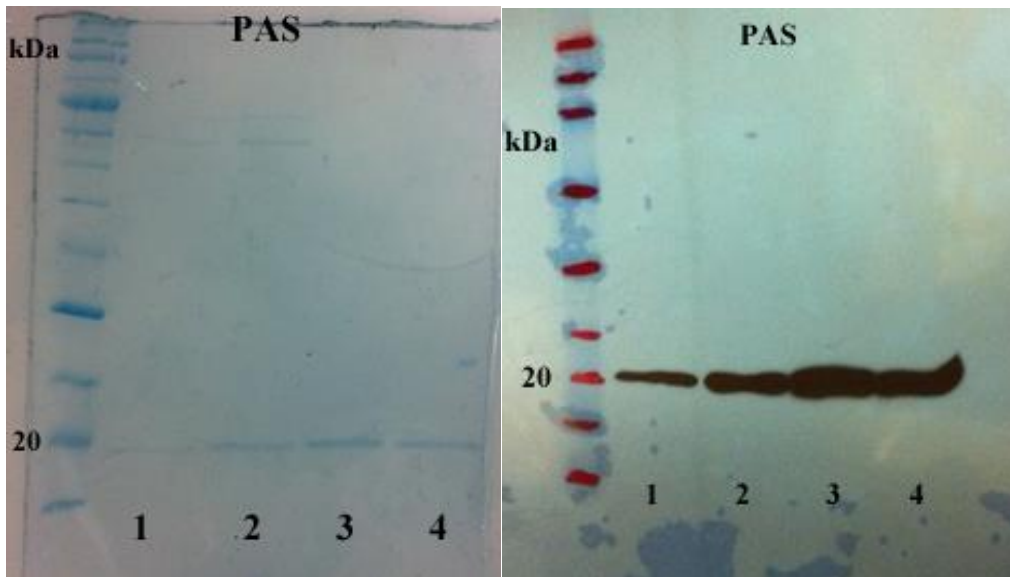


Figure 3-8. (Left) Coomassie Blue stained gel (Right) developed western blot showing an FPLC purified PAS bands. Lanes 1 and 2 correspond to peaks eluted at void volume on the FPLC. Lanes 3 and 4 are the folded proteins eluted at the working range on the FPLC.

We concentrated the PAS protein to a concentration of 8.4 μ M and used this concentration to set up several dilutions of PAS only on the AUC (Figure 3-9).

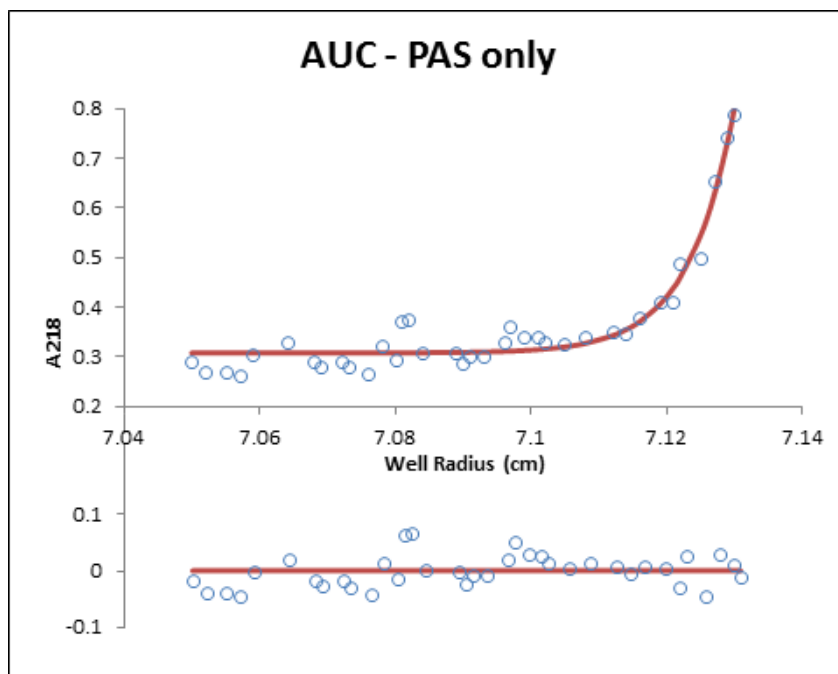


Figure 3-9. Example of a graph outputted by the AUC for the run with the PAS protein. The molecular weight of final steady-state of the equilibrium run was reported to be around 33,517 Da. This MW implied a PAS-PAS dimeric state.

An AUC run involving the PAS protein and H-NOX was also performed. The run showed results corresponding to ~30 kDa molecular weight which is the MW between a dimeric species and a monomeric state. This run will have to be repeated due to the low absorbance graph points observed when fitting the data.

GGDEF was purified using the same methods as for the other two proteins. The only difference we had to make were the induction conditions from 2XYT media to TB media; we observed very little GGDEF expression when using 2XYT induction conditions. We performed an activity assay using the initial batch of GGDEF that we purified (Figure 3-12). A western was also run to confirm the GGDEF protein (Figure 3-10).

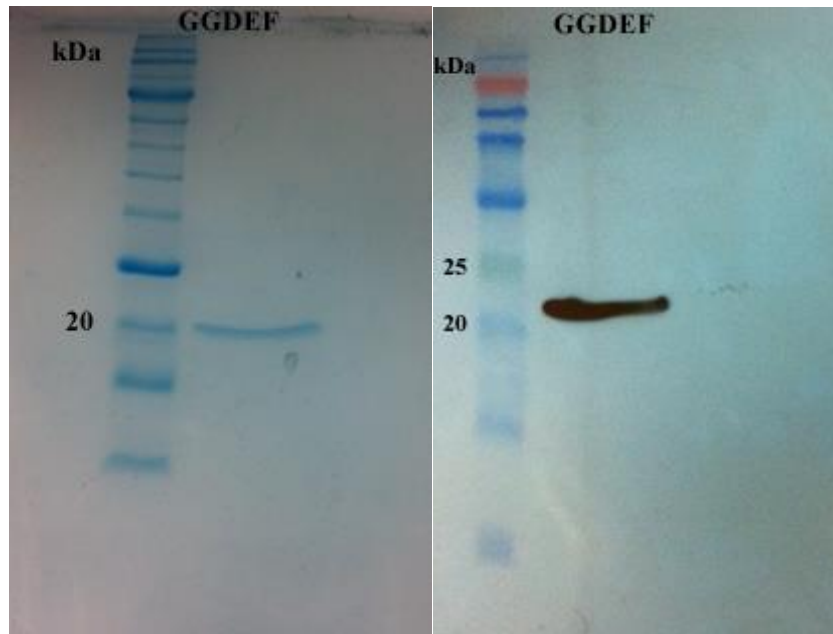


Figure 3-10. (Left) Coomassie Blue stained gel (Right) developed western blot showing an FPLC purified GGDEF band.

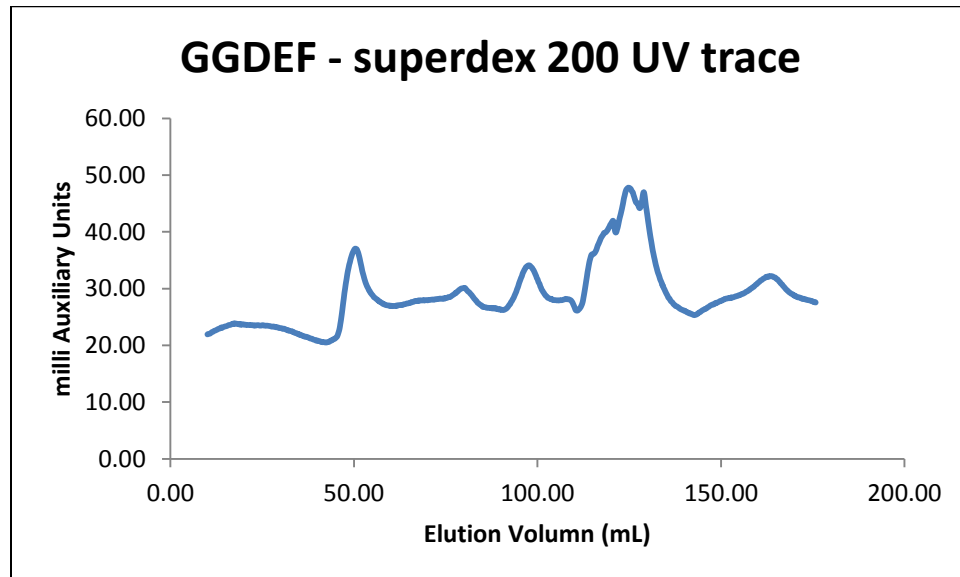


Figure 3-11. UV trace of the GGDEF profile using the FPLC system. Peak at 95ml corresponds to folded GGDEF protein.

An activity assay was set up and run using the HPLC. We incubated the enzyme with substrate (GTP) and took an initial time point. The rest of the reaction was allowed to incubate overnight at 37⁰C and was quenched the next day by boiling at 90⁰C for 5 minutes. These two

samples, the initial time point and the overnight reaction, were run along with the c-di-GMP and GTP standards on the HPLC. The graphs were exported and overlaid for comparison (Figure 3-12).

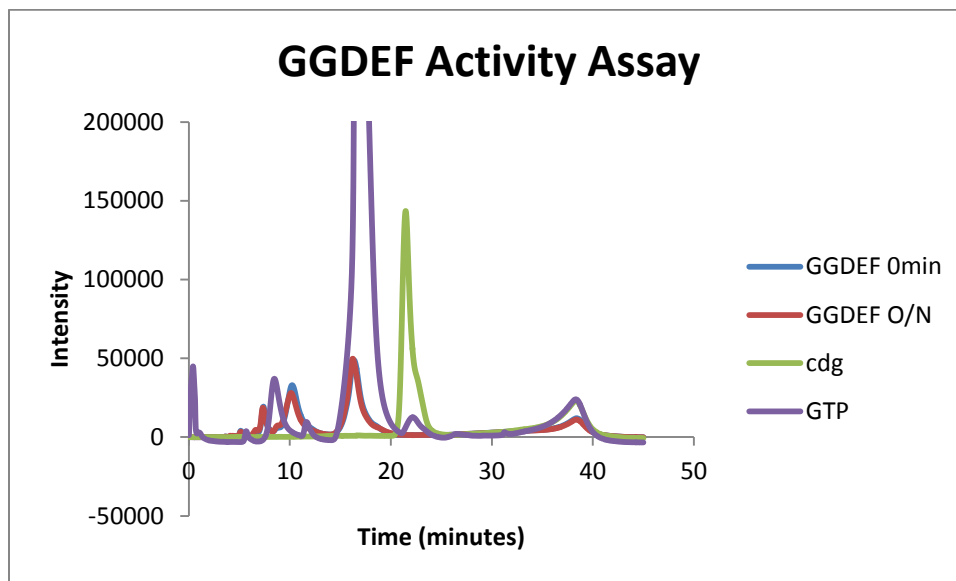


Figure 3-12. An overlay of the c-di-GMP and GTP standards along with GGDEF incubated with GTP at 0 and overnight time points on the HPLC.

Again, as with EAL, we noticed peaks being eluted at around 8 minutes that did not correspond to either of our two standards. Techniques such as mass spectroscopy would be required in order to provide additional knowledge about this chemical species. From the overlay, however, comparing the 0 and overnight time points, we see that the GTP was not degraded to any extent by the enzyme and that there is no indication of a c-di-GMP peak in the GGDEF reactions. From this we can conclude that the isolated GGDEF domain cannot maintain its activity by itself.

Although the GGDEF protein gave us no issues with the first few initial purifications, the amount of protein recovered from the working FPLC range (60ml – 110ml) started decreasing with every subsequent purification attempt. An AUC was setup with the GGDEF we initially purified, however the concentration was apparently too low for the AUC to give any usable data.

Subsequent purification attempts resulted in all of the GGDEF protein coming out at void volume (volume at which unfolded proteins emerge). Ever since then we have tried numerous methods to solve this problem including using freshly transformed cells, adding glycerol to the FPLC buffer, lowering the flow rate of the FPLC system while running the protein, etc. None of these changes had any effect on the volume at which the GGDEF protein was eluting. Due to these circumstances AUC data for the GGDEF protein is not yet available.

References

1. Kröncke, Klaus-D., Karin Fehsel, and Victoria Kolb-Bachofen. "Nitric oxide: cytotoxicity versus cytoprotection—how, why, when, and where?." *Nitric oxide* 1, no. 2 (1997): 107-120.
2. Dimmeler, Stefanie, and Andreas M. Zeiher. "Nitric oxide and apoptosis: another paradigm for the double-edged role of nitric oxide." *Nitric Oxide* 1, no. 4 (1997): 275-281.
3. Dai, Zhou, Erik R. Farquhar, Dhruv P. Arora, and Elizabeth M. Boon. "Is histidine dissociation a critical component of the NO/H-NOX signaling mechanism? Insights from X-ray absorption spectroscopy." *Dalton Transactions* 41, no. 26 (2012): 7984-7993.
4. Garg, Uttam C., and Aviv Hassid. "Nitric oxide-generating vasodilators and 8-bromo-cyclic guanosine monophosphate inhibit mitogenesis and proliferation of cultured rat vascular smooth muscle cells." *Journal of Clinical Investigation* 83, no. 5 (1989): 1774.
5. Muralidharan, Sandhya, and Elizabeth M. Boon. "Heme flattening is sufficient for signal transduction in the H-NOX family." *Journal of the American Chemical Society* 134, no. 4 (2012): 2044-2046.
6. Boon, Elizabeth M., and Michael A. Marletta. "Ligand discrimination in soluble guanylate cyclase and the H-NOX family of heme sensor proteins." *Current opinion in chemical biology* 9, no. 5 (2005): 441-446.
7. Henares, Bernadette M., Kate E. Higgins, and Elizabeth M. Boon. "Discovery of a nitric oxide responsive quorum sensing circuit in *Vibrio harveyi*." *ACS chemical biology* 7, no. 8 (2012): 1331-1336.
8. Liu, Niu, Taemee Pak, and Elizabeth M. Boon. "Characterization of a diguanylate cyclase from *Shewanella woodyi* with cyclase and phosphodiesterase activities." *Mol. BioSyst.* 6, no. 9 (2010): 1561-1564.
9. McDougald, Diane, Scott A. Rice, Nicolas Barraud, Peter D. Steinberg, and Staffan Kjelleberg. "Should we stay or should we go: mechanisms and ecological consequences for biofilm dispersal." *Nature Reviews Microbiology* 10, no. 1 (2011): 39-50.
10. Costerton, J. W., Philip S. Stewart, and E. P. Greenberg. "Bacterial biofilms: a common cause of persistent infections." *Science* 284, no. 5418 (1999): 1318-1322.
11. Makemson, John C., Nada R. Fulayfil, Warren Landry, Lisa M. Van Ert, Charles F. Wimpee, Edith A. Widder, and James F. Case. "*Shewanella woodyi* sp. nov., an exclusively respiratory luminous bacterium isolated from the Alboran Sea." *International journal of systematic bacteriology* 47, no. 4 (1997): 1034-1039.

12. Karow, David S., Duohai Pan, Rosalie Tran, Patricia Pellicena, Andrew Presley, Richard A. Mathies, and Michael A. Marletta. "Spectroscopic characterization of the soluble guanylate cyclase-like heme domains from *Vibrio cholerae* and *Thermoanaerobacter tengcongensis*." *Biochemistry* 43, no. 31 (2004): 10203-10211.
13. Liu, Niu, Yueming Xu, Sajjad Hossain, Nick Huang, Dan Coursolle, Jeffrey A. Gralnick, and Elizabeth M. Boon. "Nitric oxide regulation of cyclic di-GMP synthesis and hydrolysis in *Shewanella woodyi*." *Biochemistry* 51, no. 10 (2012): 2087-2099.
14. Yan, Hongbin, and Wangxue Chen. "3', 5'-Cyclic diguanylic acid: a small nucleotide that makes big impacts." *Chemical Society Reviews* 39, no. 8 (2010): 2914-2924.
15. Hossain, Sajjad and Elizabeth M. Boon. "Towards a Mechanistic Understanding of NO Signaling in Bacterial Group Behavior." Unpublished raw data (2013).
16. Sato, Saori, Naoya Fujita, and Takashi Tsuruo. "Modulation of Akt kinase activity by binding to Hsp90." *Proceedings of the National Academy of Sciences* 97, no. 20 (2000): 10832-10837.
17. Sukovich, David J., Jennifer L. Seffernick, Jack E. Richman, Kristopher A. Hunt, Jeffrey A. Gralnick, and Lawrence P. Wackett. "Structure, function, and insights into the biosynthesis of a head-to-head hydrocarbon in *Shewanella oneidensis* strain MR-1." *Applied and environmental microbiology* 76, no. 12 (2010): 3842-3849.
18. Kovach, Michael E., Philip H. Elzer, D. Steven Hill, Gregory T. Robertson, Michael A. Farris, R. Martin Roop II, and Kenneth M. Peterson. "Four new derivatives of the broad-host-range cloning vector pBBR1MCS, carrying different antibiotic-resistance cassettes." *Gene* 166, no. 1 (1995): 175-176.
19. Coursolle, Dan, and Jeffrey A. Gralnick. "Modularity of the Mtr respiratory pathway of *Shewanella oneidensis* strain MR-1." *Molecular microbiology* 77, no. 4 (2010): 995-1008.
20. Lebowitz, Jacob, Marc S. Lewis, and Peter Schuck. "Modern analytical ultracentrifugation in protein science: a tutorial review." *Protein Science* 11, no. 9 (2002): 2067-2079.

Appendix

Site-Directed Mutagenesis / Cloning Primers

QCCflagHnox For

5'GTTATTTTTTAATATTACACGAGCGCCTCGTGATTACAAGGATGACGATGACAAGTA
GCTCGAGGGGGGGCCCGGTACCCAGCTTTTG 3'

QCCflagHnox Rev

5'CAAAGCTGGGTACCGGGCCCCCCTCGAGCTATTGTCATCGTCATCCTTGTAATC
ACGAGGCGCTCGTGTAATATTAATAAAC 3'

QC2flagHnox For

5'GTTATTTTTTAATATTACACGAGCGCCTCGTGATTACAAGGATGACGATGACAAGTA
GTTATGAGTGCACTTGAGGACAGAG 3'

QC2flagHnox Rev

5'CTCTGTCCTCAAGTGCCTCATAACTACTTGTCATCGTCATCCTTGTAATCACGAG
GCGCTCGTGTAATATTAATAAAC 3'

QCDGCHA For

5'CATATGCAGCGCTGTATCTCTTTACCCGCTAAATACCCATACGACGTCCCAGACTA
CGCTTAGCTCGAGGGGGGGCCCGGTACCCAGCTTTTG 3'

QCDGCHA Rev

5'CAAAGCTGGGTACCGGGCCCCCCTCGAGCTAAGCGTAGTCTGGGACGTCGTAT
GGGTATTTAGCGGGTAAAGAGATACAGCGCTGCATATG 3']

KiswhnxEcofor

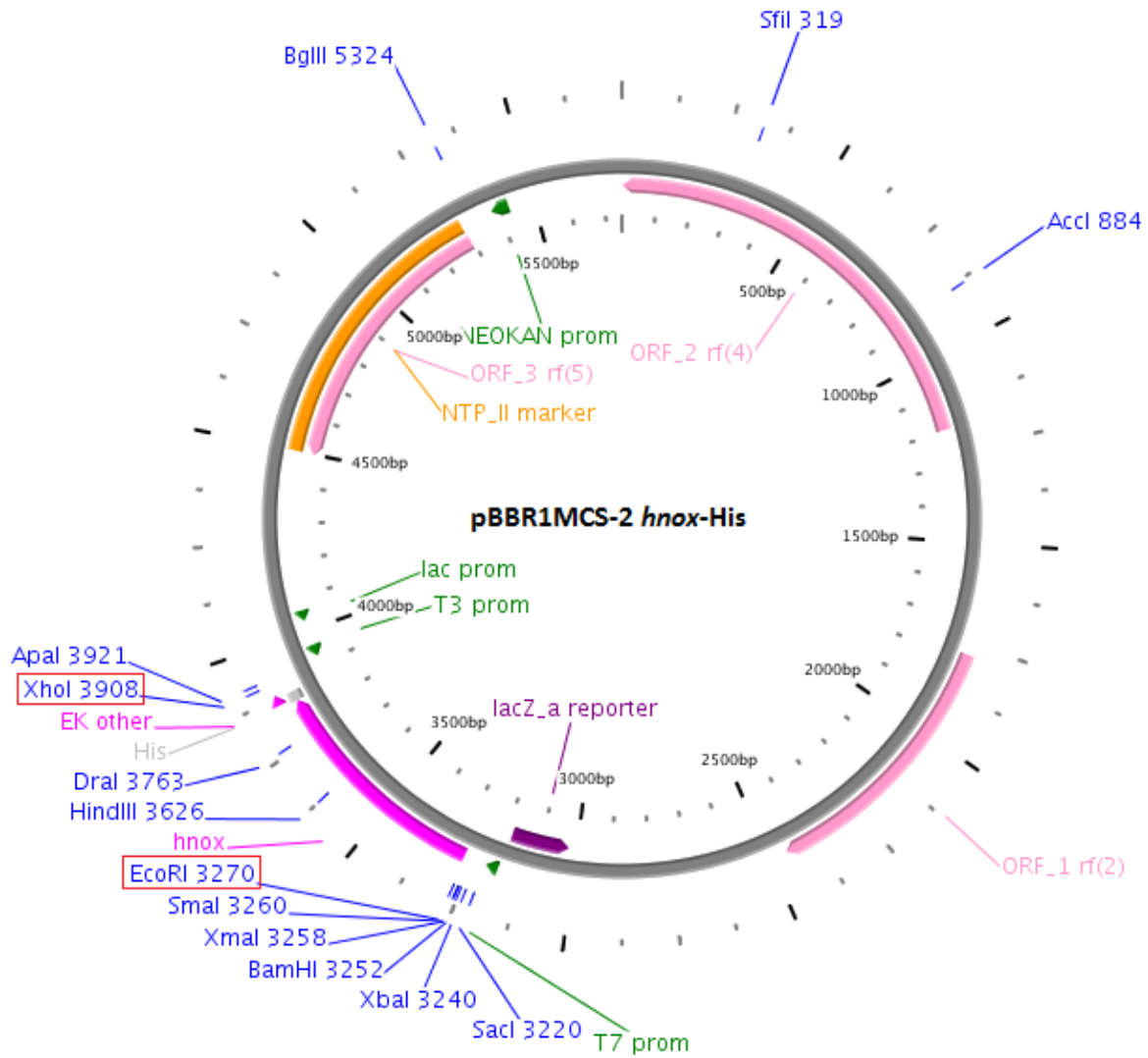
5' CAACAAGAATTCTACTTATTAACAGGGGCTAATGTTATG 3'

KiswhnxXhoRev

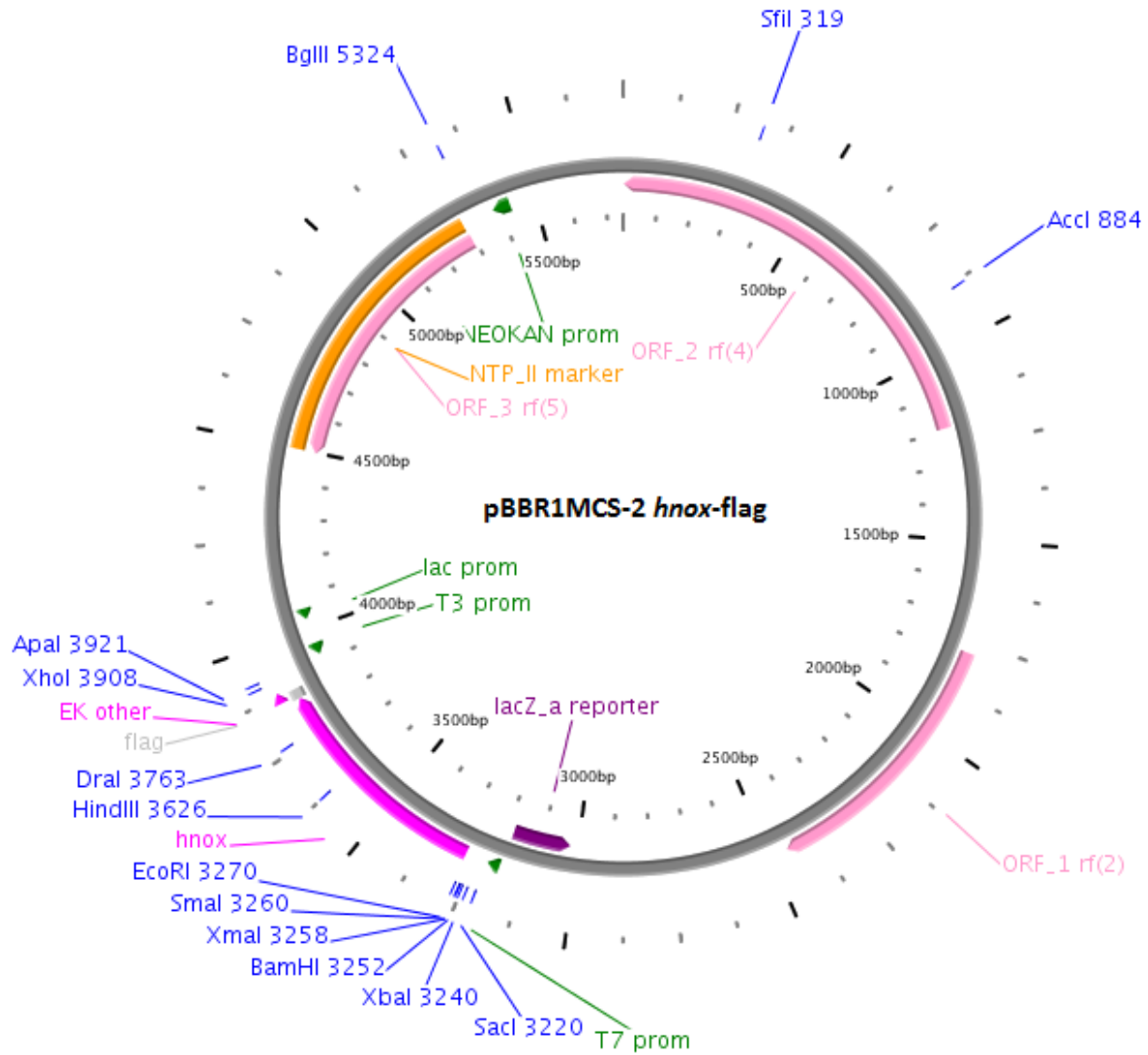
Gene Maps

All gene maps were generated using a free online vector mapper called PlasMapper (<http://wishart.biology.ualberta.ca/PlasMapper/>).

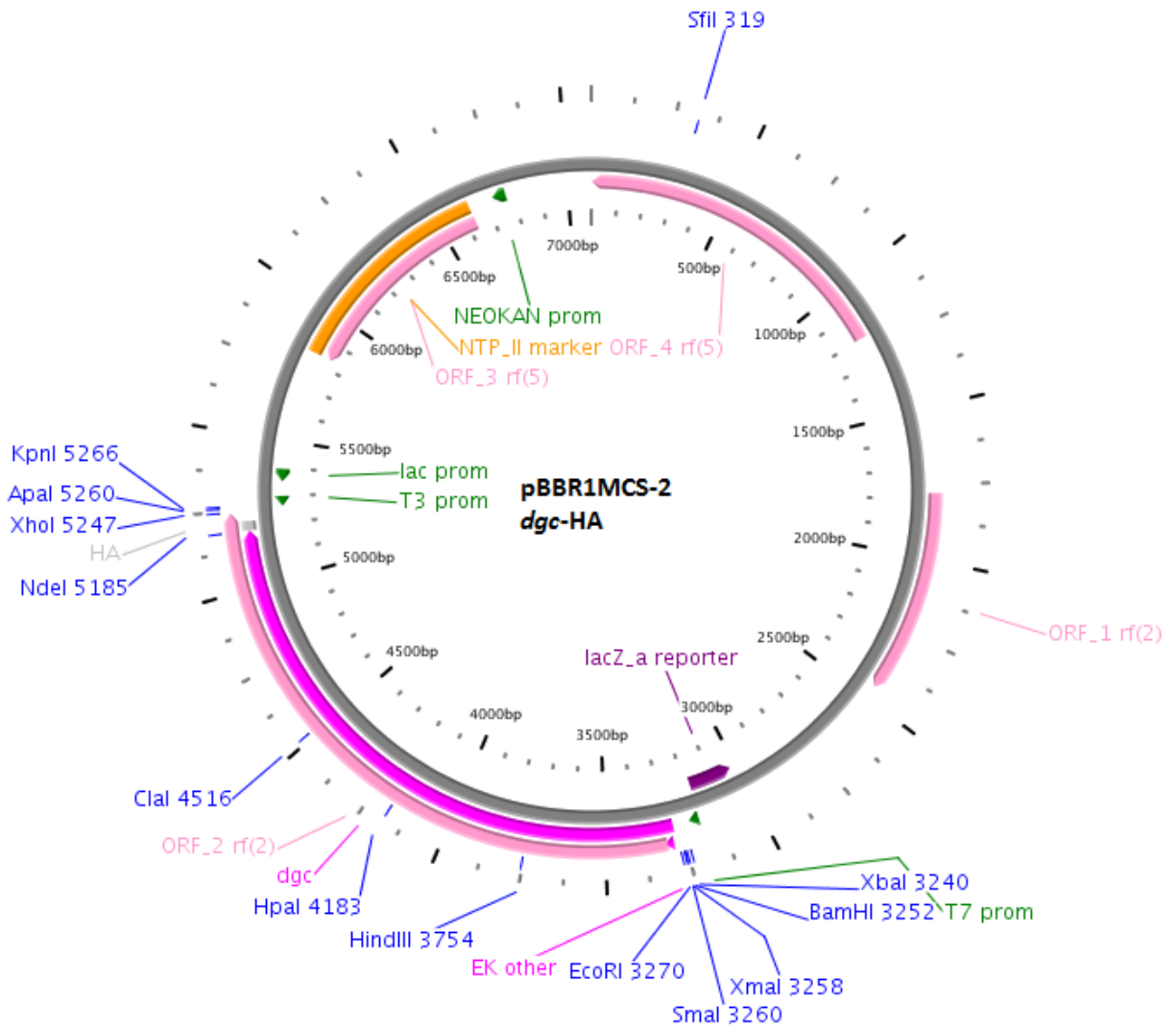
pBBR1MCS-2 *hnox*-His



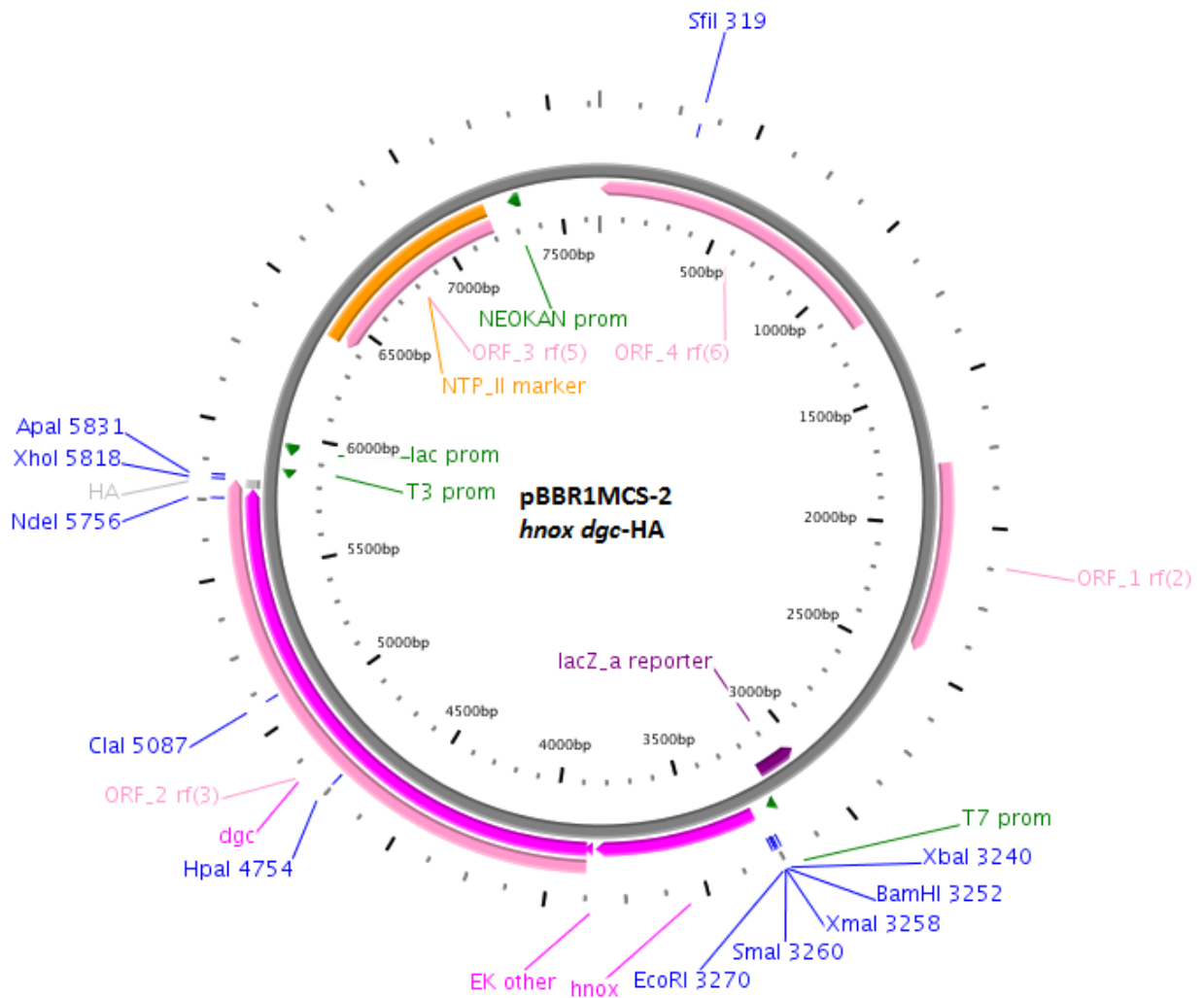
pBBR1MCS-2 *hnox*-flag



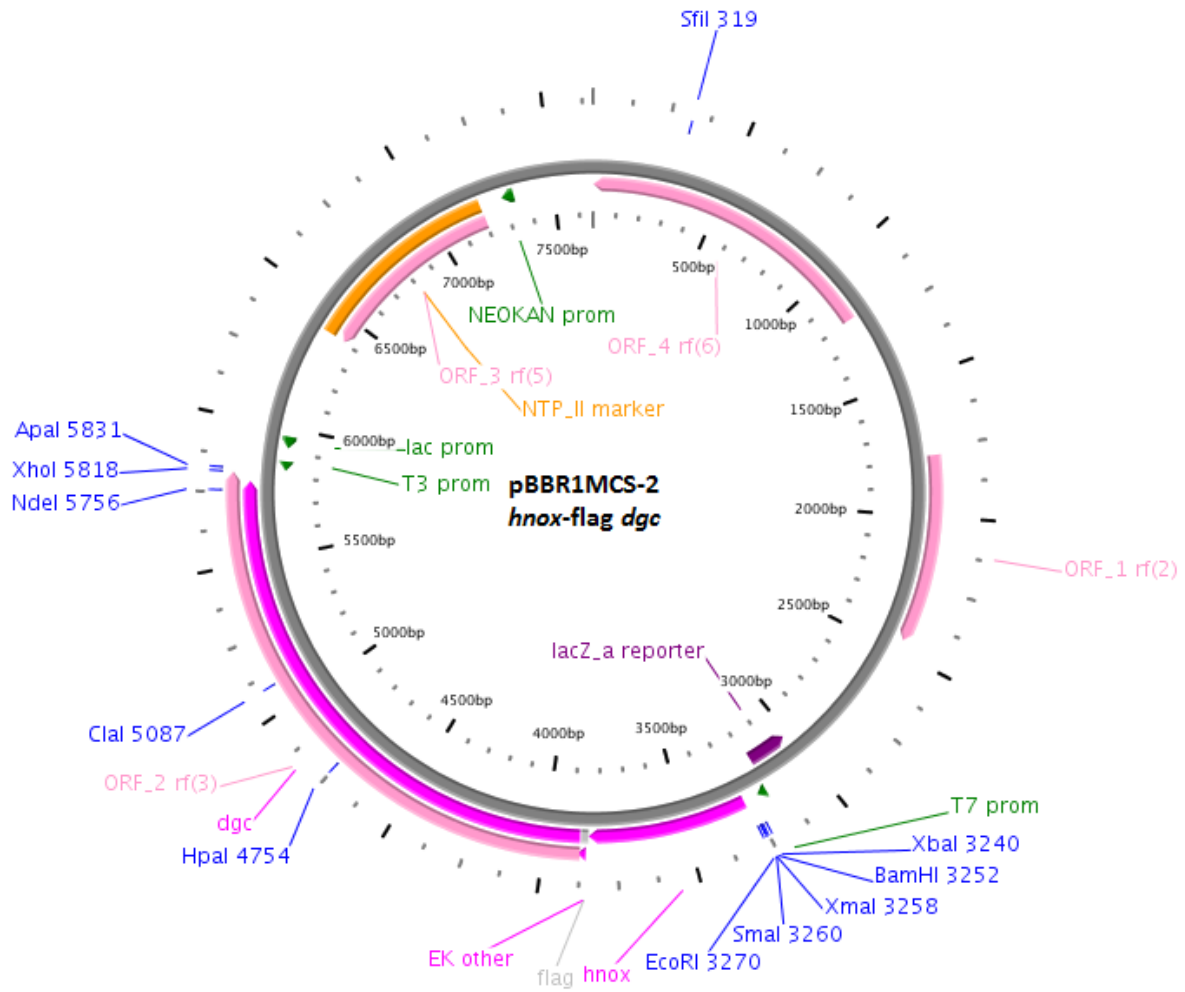
pBBR1MCS-2 *dgc*-HA



pBBR1MCS-2 *hnox dgc*-HA



pBBR1MCS-2 *hnox*-flag *dgc*



pBBR1MCS-2 *hnox*-flag *dgc*-HA

